UNIVERSITY OF CALIFORNIA
SANTA CRUZ

IMPACTS OF OCEAN ACIDIFICATION ON FORAMINIFERA AND CORALS: A FIELD STUDY

A dissertation submitted in partial satisfaction
of the requirements for the degree of

DOCTOR OF PHILOSOPHY

in

EARTH SCIENCE

by

Ana Martinez Fernandez

December 2018

The Dissertation of Ana Martinez Fernandez
is approved:

_____
Dr. Matthew Clapham, chair

_____
Dr. Adina Paytan

_____
Dr. Donald Potts

_____
Dr. Daniel Barshis

_____
Lori Kletzer
Vice Provost and Dean of Graduate Studies

Table of Contents

List of Figures

List of Tables

Abstract

IMPACTS OF OCEAN ACIDIFICATION ON FORAMINIFERA AND CORALS: A FIELD STUDY

Ana Martínez Fernández

Anthropogenic activities release CO_2 to the atmosphere, increasing the CO_2 dissolved in the ocean. This process causes a change in seawater carbonate chemistry, lowering the pH and the carbonate saturation state (Ω) and affecting marine organisms that build calcium carbonate shells and skeletons. In the last decade, an increasing concern has grown regarding the effects of ocean acidification on calcifying organisms such as foraminifera and corals. The majority of these studies are laboratory experiments or short-term field observations which do not fully reflect the complexity of natural environments and long-term ecosystem scale responses. This dissertation aims to predict the response of foraminifera and corals under future higher concentrations of atmospheric CO_2 by studying populations of benthic foraminifera and transplanted corals in natural low-pH, low-Ω springs, which constitute an *in-situ* ocean acidification laboratory.

Chapter 2 explores the impact of Ω on benthic foraminifera abundance. Foraminiferal total abundance was lower at low-Ω springs than at control sites, although symbiont-bearing and non-calcareous foraminifera were less sensitive to ocean acidification conditions than calcareous symbiont-barren foraminifera.

Chapters 3 and 4 explore the impact of Ω on coral survival, physiology and gene expression. Nubbins of *Porites astreoides, Siderastrea siderea* and *Porites porites* originating from low-Ω springs, and from ambient-Ω lagoon and reef settings were collected and transplanted to a low-Ω spring and to an ambient-Ω control site for two years. The physiological analyses suggest that slow-growing corals with high concentrations of Symbiodiniaceae, chlorophyll *a* and protein may be more resilient to ocean acidification conditions, although with reduced skeletal density. The transcriptome analysis of *P. astreoides* after one year of transplantation showed that genes involved in lipid metabolism, bicarbonate transportation and skeletal remodeling are differentially expressed at low-Ω spring transplantation site. These results suggest that corals transplanted to low-Ω spring have higher energy demands to counter the larger difference between the external seawater Ω and the internal Ω at the calcification site.

The results of this dissertation indicate that impacts of ocean acidification on benthic foraminifera and corals are species-specific, although a general negative impact on calcification and increased energy requirements are observed under low Ω conditions.

Dedication

To Mother Nature (and the organisms that perished during this research).

And to my family and friends for their unconditional support during graduate school. Muchísimas gracias.

Acknowledgements

I would like to thank my advisor Adina Paytan, for believing in me and giving me this opportunity to learn, work, travel and meet interesting people around the world. Many thanks to Paytan Lab members, your support is more than anyone could ask for, especially Abbey, Alanna, Barbara, Chia-Te, Christina, Delphine, Esra, Joe, Karen, Katie, Kim, Kyle, Nadine and Tracy.

I acknowledge my committee and co-authors Daniel Barshis, Matthew Clapham, Elizabeth Crook, Laura Hernández Terrones, Donald Potts and Mario Rebolledo Vieyra for their invaluable feedback and advice that taught me how to be a better scientist and writer.

Special thanks to Yui Takeshita and all the members of Centro de Investigación Científica de Yucatán for their help during fieldwork.

I would also like to thank all the students, staff members and professors of UCSC, Old Dominion University, Woods Hole Oceanographic Institution and Interuniversity Institute for Marine Sciences in Eilat that made my work possible.

Finally, I would like to acknowledge all the financial support I received during my stay at the University of California Santa Cruz to learn, research, and attend conferences: Argo Global grant of the Ministry of Education of Spain, Wells Fargo

Coastal Sustainability Fellowship, Hammett Environmental Studies Fellowship, UCSC Regents' Fellowship, Geological Society of America Graduate Student Research Grant, Myers Oceanographic and Marine Biology Trust Grants, International Association of Geochemistry Ph.D. Student Research Grant, Friends of Long Marine Lab Student Research and Education Award (Heald Scholarship, Norris Student Research Grant and Lillian Rouse Scholarship), Lawson Hydrology Award, UC-MEXUS Student and Postdoctoral Research Small Grant, Association for the Sciences of Limnology and Oceanography Student Travel Award, UCSC Graduate Student Association Travel Grants, National Science Foundation's International Research Experience for Students, and 7 teacher assistantships from the Earth and Planetary Science Department and 1 from the Molecular, Cell and Developmental Biology Department of UCSC.

Chapter 2 of this dissertation is a reprint of the following previously published material:

Martinez, A., Hernández-Terrones, L., Rebolledo-Vieyra, M., & Paytan, A. (2018). Impact of carbonate saturation on large Caribbean benthic foraminifera assemblages. Biogeosciences, 15(22), 6819-6832. https://doi.org/10.5194/bg-15-6819-2018. The dissertation author was the primary investigator and author of this material.

Chapter 1. Introduction

Humans are releasing increasing amounts of CO_2 through the burning of fossil fuels and deforestation. Atmospheric CO_2 dissolves in the ocean following Henry's Law and takes part in a series of chemical reactions (Eq. 1) that result in an increase in hydrogen ions concentration (a decrease in pH) and a decrease in carbonate ion (CO_3^{2-}) concentrations, a process termed ocean acidification (Caldeira & Wickett, 2003; Orr *et al.*, 2005).

$$CO_2 + H_2O \leftrightarrow H_2CO_3 \leftrightarrow HCO_3^- + H^+ \leftrightarrow CO_3^{2-} + 2H^+ \qquad \text{(Eq. 1)}$$

The ocean has already absorbed one third of the CO_2 delivered to the atmosphere by humans over the past 200 years (Sabine *et al.*, 2004), resulting in a 30% increase in hydrogen ions and a decrease of 0.1 units in surface seawater pH (Guinotte & Fabry, 2008; Raven *et al.*, 2005). Ocean pH is expected to decrease by ~ 0.4 pH units by year 2100 (Caldeira & Wickett, 2005). The protons present in seawater react with carbonate ions to form bicarbonate (Eq. 1), decreasing the concentration of carbonate ions and consequently, the carbonate saturation state of seawater.

The calcium carbonate saturation state (Ω) of seawater is defined as the ion concentration product of calcium and carbonate ions, divided by the solubility product constant (Eq. 2):

$$\Omega = \frac{[Ca^{2+}]\,[{CO_3}^{2-}]}{K_{sp}} \qquad \text{(Eq. 2)}$$

Since calcium concentrations are relatively constant in the oceans, the Ω depends predominantly on the carbonate ions concentration. Many marine organisms produce calcium carbonate shells and skeletons in the form of aragonite (orthorhombic symmetry) and calcite (trigonal symmetry). Therefore, a decrease in seawater carbonate ion concentration lowers the calcium carbonate saturation state, affecting the biosynthesis of calcium carbonate (Smith & Buddemeier, 1992). Ocean acidification may also affect other physiological processes like reproduction, communication, or gas exchange (Fabry *et al.*, 2008; Raven *et al.*, 2005).

Foraminifera and corals are calcifying organisms that provide substantial ecosystem services such as protection from erosion and formation of the coastal relief and sand beaches, in addition to serving as a carbon sink (on geological time scales) and as a habitat and food for many other marine organisms. Therefore, a reduction in health and survival of these organisms will have important consequences in the whole ecosystem, social impacts on human populations living in coastal areas as well as economic impacts on local fisheries and tourism activities.

Most of the research carried out to date to assess the effects of ocean acidification on foraminifera and corals has been performed through experiments in a laboratory, controlling different parameters such as partial pressure of CO_2 or alkalinity (Chan & Connolly, 2013; Doo *et al.*, 2014; Keul *et al.*, 2013; Kroeker *et al.*, 2010). While informative, these experiments do not completely reflect the effects of carbonate chemistry change over a long period of time or complex natural variability and

ecosystem interactions. This dissertation studies the effects of ocean acidification on calcifying organisms from an *in-situ* perspective, where observations or *in-situ* manipulations are conducted along natural Ω gradients close to low-Ω submarine springs.

The low-Ω springs (locally called "ojos") are located along the east coast of Yucatan Peninsula (Quintana Roo, Mexico). The Yucatan Peninsula is a karstic region where the rainfall percolates rapidly into the ground, creating a groundwater system that discharges brackish low-pH, low-Ω groundwater to the Caribbean Sea, close to the Mesoamerican Barrier Reef System. Thirteen ojos have been extensively studied in Puerto Morelos (Crook *et al.*, 2012; Crook *et al.*, 2013; Crook *et al.*, 2016; Hofmann *et al.*, 2011; Null *et al.*, 2014; Paytan *et al.*, 2014); they are located inside the reef lagoon, 500 m offshore, occurring as small seeps or long fractures at depths of less than 7 meters. This system is not an exact analogue to the oceans in a future with high CO_2 levels, as the alkalinity and total inorganic carbon of the discharging water are higher than ambient seawater, while salinity is slightly lower. Nevertheless, species living there have been exposed to low-Ω conditions for their entire lifespans, creating a unique setting to study ocean acidification effects in a natural setting that has existed for thousands of years.

In chapter 2, I study the absolute and relative abundance of benthic foraminifera with distinct feeding strategies and secreting different shell types near 5 ojos and respective control sites to determine foraminifera species response to low Ω. In chapter

3, I explore the survival and phenotypical changes of three coral species after two years of transplantation to a low-Ω spring to understand the impacts of ocean acidification on calcification and physiology. In chapter 4, I research the gene expression of the coral *Porites astreoides* after one year of transplantation to a low-Ω spring to understand the molecular mechanisms involved in coral calcification at *in-situ* ocean acidification conditions.

Chapter 2. Impact of carbonate saturation on large Caribbean benthic foraminifera assemblages

Ana Martinez[1], Laura Hernández-Terrones[2], Mario Rebolledo-Vieyra[3], Adina Paytan[4]

[1] Department of Earth and Planetary Sciences, University of California Santa Cruz, 1156 High Street, Santa Cruz, CA 95064, USA

[2] Universidad del Caribe, L-1. Mz 1, Esq. Fracc. Tabachines SM 78, Cancún, Quintana Roo, 77528, México

[3] Chipre 5, Resid. Isla Azul, Cancún, Quintana Roo, 77500, México

[4] Institute of Marine Science, University of California Santa Cruz, Santa Cruz, CA 95064, USA

Abstract

Increasing atmospheric carbon dioxide and its dissolution in seawater have reduced ocean pH and carbonate ion concentrations, with potential implications on calcifying organisms. To assess the response of large Caribbean benthic foraminifera to low carbonate saturation conditions, we analyzed benthic foraminifers' abundance and relative distribution in surface sediments in proximity to low-carbonate saturation submarine springs and at adjacent control sites. Our results show that the total abundance of large benthic foraminifera was significantly lower at the low-pH submarine springs than at control sites, although responses were species specific. The relative abundance of high-magnesium, porcelaneous foraminifera was higher than that of hyaline foraminifera at the low-pH springs due to the abundant *Archaias angulatus*, a chlorophyte-bearing foraminifer, which secretes a large and robust test that is more resilient to dissolution at low-calcite saturation. The different assemblages found at the submarine springs indicate that calcareous symbiont-barren foraminifera are more sensitive to the effects of ocean acidification than agglutinated and symbiont-bearing foraminifera, suggesting that future ocean acidification will likely impact natural benthic foraminifera populations.

2.1 Introduction

Anthropogenic activities such as deforestation and fossil fuel burning are increasing the concentration of carbon dioxide (CO_2) in the atmosphere. About one third of all the CO_2 emitted into the atmosphere by humans over the past 200 years has been absorbed by the oceans (Sabine *et al.*, 2004), causing a change in ocean chemistry, lowering the pH and the concentration of carbonate ions in seawater, collectively referred to as ocean acidification. It is expected that ocean pH will decrease even more, by ~ 0.4 pH units by year 2100 (Caldeira & Wickett, 2003; Orr *et al.*, 2005) with possible consequences to marine organisms and ecosystems (Raven *et al.*, 2005). Marine calcifying organisms may be particularly sensitive due to the lower availability of carbonate ions, which are required for their shell formation (Raven *et al.*, 2005).

Foraminifera are single-celled organisms that are abundant in the marine water column and sediments, playing key roles in many marine ecosystems, including being basal contributors to the marine food web and essential elements of the marine carbonate pump (Culver & Lipps, 2003; Hain *et al.*, 2014; Legendre & Le Fèvre, 1995). Calcareous foraminifera produce calcium carbonate tests of diverse shapes and thickness, while agglutinated foraminifera build a test made of detrital particles, and thecate foraminifera lack a test. The calcification pathway and magnesium content of calcareous foraminifera varies between perforate hyaline and imperforate porcelaneous foraminifera (Brasier, 1980). Some large benthic foraminifera harbor photosynthetic algal symbionts, while others rely solely on heterotrophic feeding (Murray, 1991). The diversity of lifestyles and test characteristics suggest that the sensitivity of this group

of organisms to changing ocean carbonate chemistry will be species dependent (Fabry *et al.*, 2008; Fujita *et al.*, 2011).

Laboratory culture experiments where benthic foraminifera were maintained under controlled conditions (i.e., partial pressure of CO_2, alkalinity, etc.) generally showed a decline in foraminifera calcification under high pCO_2 (Erez, 2003; Haynert *et al.*, 2011; Keul *et al.*, 2013). However, this response was not uniform and varied among species (Fujita *et al.*, 2011; Hikami *et al.*, 2011; McIntyre-Wressnig *et al.*, 2013). Field studies at CO_2 vents in the Pacific Ocean (Fabricius *et al.*, 2011; Uthicke *et al.*, 2013) and Mediterranean Sea (Dias *et al.*, 2010) reported a decrease in benthic foraminiferal abundance with increasing pCO_2, especially of calcareous species; nonetheless benthic foraminifera have been found living near CO_2 vents in the northern Gulf of California (Pettit *et al.*, 2013) and near experimentally injected deep-sea CO_2 hydrate (Bernhard *et al.*, 2009), and generally, foraminifera can be found in a wide range of environments (Brasier, 1980).

To shed light on the potential response of large Caribbean benthic foraminifera to a future increase in CO_2 concentration and an associated decrease in pH and carbonate ion concentrations, we studied the absolute and relative abundance of large benthic foraminifera around a series of submarine springs that naturally discharge low-carbonate saturation state (Ω) saline groundwater in the Yucatán Peninsula, Mexico (Crook *et al.*, 2012). The Yucatán Peninsula is a karstic region with extensive nearshore submarine groundwater springs that discharge water characterized by low pH, high

total inorganic carbon, and total alkalinity, but it has only slightly lower salinity and similar temperatures to local marine conditions (Crook *et al.*, 2012; Crook *et al.*, 2013; Crook *et al.*, 2016; Hofmann *et al.*, 2011; Null *et al.*, 2014; Paytan *et al.*, 2014). Previous studies have determined that the springs have been discharging low-Ω water for millennia (Back *et al.*, 1979); therefore, they serve as a natural laboratory to study the *in-situ* responses of marine organisms and ecosystems to long-term exposure to low Ω, which may not be captured in short-term experiments (Andersson *et al.*, 2015). Field studies from this site reported reduced coral species richness and coral colony size at the springs, compared to control sites (Crook *et al.*, 2012), and a 70% smaller cover of calcifying benthic organisms after 14 months of a recruitment experiment (Crook *et al.*, 2016). We hypothesize that benthic foraminifera assemblages will also differ between the springs and control sites, decreasing in overall abundance and having distinct species composition depending on test type, magnesium content, feeding strategy, and the photosymbiotic associations of foraminifera.

2.2 Materials and methods

2.2.1 Field sampling

Benthic foraminifera from the upper centimeter of sediment were collected in October 2011 near five submarine groundwater springs (Norte, Mini, Pargos, Laja, and Gorgos) at Puerto Morelos reef lagoon (National Marine Park), in the Mexican Caribbean coast off of Quintana Roo (Fig. 2.1). At each spring site, five replicates of surface sediment samples (coarse sand) were collected using a spoon into centrifuge tubes, from near the center of the submarine spring and at five control sites about two

meters away from each spring, outside the impact area of the spring. Water samples were also collected at each site.

2.2.2 Water chemistry

Water temperature and pH were measured *in-situ* with a handheld YSI analyzer (Yellow Springs model 63). Seawater samples were filtered (0.2 μm filter) and split into aliquots for total inorganic carbon (C_T), total alkalinity (A_T), and salinity measurements following the standard operating procedures described by Dickson *et al.* (2007). Total inorganic carbon was analyzed on a CM5011 Carbon Coulometer (UIC, Inc.; analytical measurement error: ±3 μ mol kg^{-1}). Total alkalinity was measured using an automated open-cell, potentiometric titrator (Orion model 950; analytical measurement error: ±2 μ mol kg^{-1}). Certified CO_2 reference material (from A. Dickson lab at UC San Diego, batch 112) was used to calibrate the instruments. Salinity was analyzed using a portable salinometer (Portasal Model 8410, Guild Line). The program CO_2Sys (Pierrot *et al.*, 2006) was used to calculate pH, carbonate ion concentrations, and the Ω of seawater (CO_2 dissociation constants –Lueker *et al.* (2000); $KHSO_4$ – Dickson *et al.* (2007); B concentration –Uppström (1974)).

2.2.3 Foraminiferal analysis

Five replicate sediment samples per site were freeze dried, weighed, washed with deionized water through a 63 μm sieve to remove clay and silt, dried at 50° C, and the > 250 μm fraction was analyzed under an optical microscope (Bausch and Lomb) to determine foraminiferal abundance measured as individuals per gram of sediment.

The > 250 μm fraction contains the assemblage of adult individuals that are likely to be conserved in the sediment (Martin, 1986). Small juveniles of species dominating the shallow coastal setting have high mortality rates (pre-reproductive death rate of 99.5% for *A. angulatus* – Knorr *et al.*, 2015; > 99% for *Amphistegina* spp. – Muller, 1974), and mortality rates of large foraminifera drop once their diameter is ~ 0.5 mm (Hallock & Glenn, 1986). Specifically, in our samples the > 250 μm fraction typically constituted > 80% of the total tests in a sample. Indeed, large-size foraminifera are typical to warm, oligotrophic, well-lit, shallow-water assemblages (Hallock, 1985). At least 1 g of sediment per replicate was analyzed (with 2 g per replicate for most samples). At least 300 individuals per replicate were counted; however, in 24 of the 50 samples less than 300 individuals per replicate were counted due to low foraminifera abundance. Foraminifera were identified following several taxonomic references (Crevison & Hallock, 2001; d'Orbigny, 1839; Poag, 1981; Wantland, 1967); each individual within a genus was counted and total foraminiferal and genus abundances were normalized to sediment weight. Only the most common genera (> 5% of the assemblage in 10% of the samples) were counted and considered for statistical analyses.

2.2.4 Test weight

Tests of *Discorbis rosea* from the 250 –355 μm sediment size fraction (2 to 122 individuals) were weighted using an analytical microbalance (Sartorius, model CP2P, ±5 μg error), and average weight per specimen was determined. This species was chosen because of its abundance in most of the samples and the relatively constant test size.

2.2.5 Statistical analysis

Data analysis and visualization were performed using R program version 3.4.3 (Team, 2015) and the "vegan" package in R (Oksanen *et al.*, 2013). A non-parametric Mann–Whitney rank sum test was conducted to determine differences in foraminiferal abundance and weight between each low-Ω submarine spring and its corresponding control site. A permutational multivariate analysis of variance (PERMANOVA, 9999 permutations) was used on the Bray–Curtis dissimilarity matrix after the square-root-transformed relative abundance of foraminifera to test for differences in community structure between saturation states and sites. Similarity percentages analysis (SIMPER) was used to determine the most important genera that contributed to dissimilarities in community structure. Non-metric multidimensional scaling (nMDS) ordination was used to visualize the similarity in foraminiferal assemblages among Ω levels and sites. nMDS plots were created with the metaMDS function on the Bray–Curtis dissimilarity matrix of foraminiferal relative abundances and constrained to two dimensions. To evaluate the effects of environmental variables on foraminiferal relative abundance, the log-transformed water chemistry data were overlaid using the envfit function of the vegan library (Dixon, 2003) with 9999 permutations.

2.3 Results

2.3.1 Water chemistry

The Ω, pH, and salinity of water in all springs was lower than their corresponding control sites (Table 2.1), while alkalinity (A_T) and total inorganic carbon (C_T) were higher than control sites. Temperature (T) was similar at all locations. These

data represent the analyses of discrete water samples collected during sediment sampling; more data, including continuous data collected by deployed sensors at some of these sites, have been previously published (Crook *et al.*, 2012; Crook *et al.*, 2013; Crook *et al.*, 2016; Hofmann *et al.*, 2011; Null *et al.*, 2014; Paytan *et al.*, 2014), and data reported here are within the range of the published data. The specific spring sites were selected because the salinity at these sites is > 30 over 90% of the time and does not drop below 27; when salinity drops below 30 (7% of the time), the low-salinity exposure lasts for very short periods of time, always less than 1 h (Crook *et al.*, 2013).

2.3.2 Absolute abundance of foraminifera

The absolute abundance of foraminifera measured as total number of individuals per gram of sediment was higher at high-Ω control sites than at low-Ω springs in Norte ($W = 25$, $p < 0.01$), Mini ($W = 25$, $p < 0.01$), Pargos ($W = 25$, $p < 0.01$), and Laja ($W = 25$, $p < 0.01$), but not in Gorgos ($W = 21$, $p = 0.095$; Fig. 2.2).

2.3.3 Genus assemblage

The seven most abundant genera were: *Amphistegina*, *Archaias*, *Asterigerina*, *Quinqueloculina*, *Triloculina*, *Discorbis*, and *Gaudryina*. Other foraminifera that were present in some of the samples at a smaller abundance (< 5% of assemblage) belong to the following genera: *Borelis*, *Clavulina*, *Elphidium*, *Spiroloculina*, *Peneroplis*, *Laevipeneroplis*, *Planorbulina*, *Sorites*, *Vertebralina*, and *Heterostegina*. The composition of foraminifera communities (relative abundance of genera) changed significantly between saturation states ($PERMANOVA_{saturation}$: $F_{1,50} = 12.11$, $p <$

0.0001) and between sites ($PERMANOVA_{site}$: $F_{4,50} = 8.15$, $p < 0.0001$). A SIMPER analysis revealed that *Archaias* and *Discorbis* genera contributed the most to dissimilarities in community structure between low Ω and high Ω in most of the sites, while *Asterigerina* contributed the most in Pargos (Fig. 2.3). *Archaias* relative abundance increased at low Ω, and *Discorbis* and *Asterigerina* relative abundances decreased at low Ω in all sites. *Amphistegina* and *Gaudryina* relative abundances increased at low Ω in all sites but Norte. *Quinqueloculina* and *Triloculina* combined relative abundance decreased at low Ω in Pargos, Laja, and Gorgos and increased in Norte and Mini.

2.3.4 Foraminifera test type

Foraminifera were divided into three groups to investigate abundance differences based on test type. The calcareous porcelaneous group included *Archaias angulatus* and several species of *Quinqueloculina* and *Triloculina* genera. The calcareous hyaline group included *Amphistegina*, *Asterigerina*, and *Discorbis*. The non-calcareous agglutinated group included individuals of the genus *Gaudryina*. Porcelaneous absolute abundance was lower at low Ω at all sites but Gorgos (see Fig. 2.4 – Norte: $W = 23$, $p < 0.05$; Mini: $W = 25$, $p < 0.01$; Pargos: $W = 25$, $p < 0.01$; Laja: $W = 25$, $p < 0.01$; Gorgos: $W = 20$, $p = 0.151$). Hyaline absolute abundance was lower at low Ω at all sites (Norte: $W = 25$, $p < 0.01$; Mini: $W = 25$, $p < 0.01$; Pargos: $W = 25$, $p < 0.01$; Laja: $W = 25$, $p < 0.01$; Gorgos: $W = 25$, $p < 0.01$). The absolute abundance of agglutinated foraminifera was lower at low Ω than at high Ω in Norte ($W = 24$, $p < 0.05$) and Mini ($W = 25$, $p < 0.01$) and did not vary with Ω in Pargos ($W = 16$, $p =$

0.548), Laja (W = 21, p = 0.095), and Gorgos (W = 11, p = 0.841). The relative abundance of foraminifera measured as a percentage of each group within the population also differed between Ω conditions (Fig. 2.4). Porcelaneous relative abundance was higher at low Ω in Norte and Laja (Norte: W = 0, p < 0.01; Mini: W = 5, p = 0.151; Pargos: W = 5, p = 0.151; Laja: W = 0, p < 0.01; Gorgos: W = 5, p = 0.142). In contrast, the hyaline relative abundance was lower at low Ω in Norte and Laja (Norte: W = 25, p < 0.01; Mini: W = 20, p = 0.142; Pargos: W = 20, p = 0.151; Laja: W = 25, p < 0.01; Gorgos: W = 20, p = 0.151). The relative abundance of agglutinated foraminifera was higher at low Ω in Laja (W = 2, p < 0.05) and did not vary with Ω in the other four sites (Norte: W = 16, p = 0.548; Mini: W = 6, p = 0.222; Pargos: W = 3, p = 0.056; Gorgos: W = 7, p = 0.310).

2.3.5 Effect of magnesium content in test of calcareous foraminifera

Calcareous foraminifera were divided into three groups based on the magnesium (Mg) content of their test to evaluate the effect of Mg-dependent solubility on abundance. Foraminifera were grouped into low-Mg-content (*Discorbis*), intermediate-Mg-content (*Amphistegina* and *Asterigerina*), and high-Mg-content (*Archaias*, *Quinqueloculina* and *Triloculina*) tests. The absolute abundance of foraminifera with a low-Mg test was lower at low Ω in all sites (see Fig. 2.5 – Norte: W = 25, p < 0.01; Mini: W = 25, p < 0.01; Pargos: W = 25, p < 0.01; Laja: W = 25, p < 0.01; Gorgos: W = 25, p < 0.01). Similarly, the absolute abundance of intermediate-Mg foraminifera was lower at low Ω in all sites (Norte: W = 25, p < 0.01; Mini: W = 25, p < 0.01; Pargos: W = 25, p < 0.01; Laja: W = 25, p < 0.01; Gorgos: W = 23, p <

0.05). The absolute abundance of high-Mg foraminifera was lower at low Ω at all sites but Gorgos (Norte: W = 23, $p < 0.05$; Mini: W = 25, $p < 0.01$; Pargos: W = 25, $p < 0.01$; Laja: W = 25, $p < 0.01$; Gorgos: W = 20, $p = 0.151$).

The relative abundance of low-Mg foraminifera was lower at low Ω in Norte, Mini, and Laja (Norte: W = 25, $p < 0.01$; Mini: W = 25, $p < 0.01$; Pargos: W = 20, $p = 0.151$; Laja: W = 25, $p < 0.01$; Gorgos: W = 20, $p = 0.151$). The relative abundance of intermediate-Mg foraminifera was significantly lower at low Ω in Norte and Pargos (Norte: W = 25, $p < 0.01$; Mini: W = 8, $p = 0.421$; Pargos: W = 23, $p < 0.05$; Laja: W = 18, $p = 0.309$; Gorgos: W = 20, $p = 0.151$). In contrast, the relative abundance of high- Mg foraminifera was higher at low Ω in Norte and Laja (Norte: W = 0, $p < 0.01$; Mini: W = 5, $p = 0.142$; Pargos: W = 5, $p = 0.151$; Laja: W = 0, $p < 0.01$; Gorgos: W = 5, $p = 0.151$).

2.3.6 Feeding strategy of calcareous foraminifera

Calcareous foraminifera were divided into two groups based on their feeding strategy: heterotrophic-symbiont-barren foraminifera, and symbiont-bearing foraminifera. The absolute abundance of calcareous heterotrophic foraminifera was lower at low Ω than at high Ω at all sites but Gorgos (see Fig. 2.6 – Norte: W = 25, $p < 0.01$; Mini: W = 25, $p < 0.01$; Pargos: W = 25, $p < 0.05$; Laja: W = 25, $p < 0.01$; Gorgos: W = 20, $p = 0.151$). The absolute abundance of symbiont-bearing foraminifera was also lower at low Ω than at high Ω at all sites but Gorgos (Norte: W = 24, $p < 0.05$; Mini: W = 25, $p < 0.01$; Pargos: W = 25, $p < 0.01$; Laja: W = 25, $p < 0.01$; Gorgos: W = 19,

p = 0.222). The relative abundance of heterotrophic foraminifera was lower at low Ω than at high Ω in all sites but Gorgos (Norte: W = 25, p < 0.01; Mini: W = 25, p < 0.01; Pargos: W = 25, p < 0.01; Laja: W = 25, p < 0.01; Gorgos: W = 20, p = 0.151). In contrast, the relative abundance of symbiont-bearing foraminifera was higher at low Ω at all sites but Gorgos (Norte: W = 0, p < 0.01; Mini: W = 0, p < 0.01; Pargos: W = 0, p < 0.01; Laja: W = 0, p < 0.01; Gorgos: W = 5, p = 0.151).

2.3.7 Symbiont type of calcareous foraminifera

To test the differences among symbiont types on foraminifera abundance with respect to Ω, symbiont-bearing foraminifera were divided into two groups: diatom-bearing foraminifera (*Amphistegina* and *Asterigerina*) and chlorophyte-bearing foraminifera (*Archaias*). The absolute abundance of diatom-bearing foraminifera was lower at low Ω at all sites (see Fig. 2.7 – Norte: W = 25, p < 0.01; Mini: W = 25, p < 0.01; Pargos: W = 25, p < 0.01; Laja: W = 25, p < 0.01; Gorgos: W = 23, p < 0.05). The absolute abundance of chlorophyte-bearing foraminifera was lower at low Ω in Mini, Pargos, and Laja and did not vary significantly in Norte and Gorgos (Norte: W = 20, p = 0.151; Mini: W = 25, p < 0.01; Pargos: W = 24, p < 0.05; Laja: W = 25, p < 0.01; Gorgos: W = 12, p = 0.1).

The relative abundance of diatom-bearing foraminifera was lower at all sites but Mini (Norte: W = 25, p < 0.01; Mini: W = 17, p = 0.421; Pargos: W = 24, p < 0.05; Laja: W = 25, p < 0.01; Gorgos: W = 25, p < 0.01). Contrastingly, the relative abundance of chlorophyte-bearing foraminifera was higher at all sites but Mini (Norte:

W = 0, $p < 0.01$; Mini: W = 8, $p = 0.421$; Pargos: W = 1, $p < 0.05$; Laja: W = 0, $p < 0.01$; Gorgos: W = 0, $p < 0.01$).

2.3.8 Environmental factors

The nMDS plots showed a clear clustering of relative abundances between high and low Ω, while this clustering was not apparent between sites at a specific saturation state (Fig. 2.8). The envfit function revealed that areas where calcareous heterotrophic foraminifera were relatively more abundant are the control sites, which are characterized by higher pH ($R^2 = 0.3531$, $p = 0.001$), salinity ($R^2 = 0.4420$, $p = 0.001$), and Ω (represented as the arrow titled calcite in Fig. 2.8, $R^2 = 0.4735$, $p = 0.001$), while the areas where calcareous heterotrophic foraminifera were less abundant are the spring sites, which are characterized by higher alkalinity (represented as arrow A in Fig. 2.8; $R^2 = 0.4420$, $p = 0.001$) and higher total inorganic carbon (represented as arrow C in Fig. 2.8; $R^2 = 0.4261$, $p = 0.001$). Calcareous symbiont-bearing foraminifera were relatively more abundant in low-Ω areas (blue symbols) with higher temperatures (represented as arrow T in Fig. 2.8; $R^2 = 0.1234$, $p = 0.036$), although the temperature is not on the main gradient of variation, and the difference among sites was at most 2°C, which is lower than diurnal or seasonal natural variability within sites. The relative abundance of agglutinated foraminifera was not affected by the main gradient explaining the maximal variance of data. These trends are consistent with field observations.

2.3.9 Test weight

The average test weights of *Discorbis rosea* (size fraction 250–355 μm) did not differ among saturation states in any of the sites (Norte: W = 13, p = 0.1; Mini: W = 13, p = 0.2; Pargos: W = 7, p = 0.309; Laja: W = 8, p = 0.421; Gorgos: W = 20, p = 0.151 – see Fig. 2.9).

2.4 Discussion

2.4.1 Absolute abundance of calcifying benthic foraminifera decreases at low Ω springs

The analysis of foraminiferal abundance in surface sediments collected from low Ω submarine springs and control sites revealed that the absolute abundance of calcareous foraminifera was lower at springs than at control sites (Fig. 2.2). Calcification of calcareous foraminifera is a process that depends on the carbonate chemistry of seawater and requires calcite-supersaturated conditions at the calcification site (Bentov *et al.*, 2009; Erez, 2003). Foraminifera endocytosis of seawater occurs to bring calcium and inorganic carbon to the active calcification site (Bentov *et al.*, 2009). In the process, the vacuolated seawater is alkalinized to a pH of ~ 9 to overcome the magnesium-mediated inhibition of calcite precipitation and to promote the conversion of inorganic carbon from bicarbonate to carbonate ions (de Nooijer *et al.*, 2009).This pH elevation at the site of calcification is achieved by using ATP to pump protons out of the foraminifera protoplasm (Glas *et al.*, 2012; Toyofuku *et al.*, 2017). If the ambient pH is low, the foraminifera have to devote more energy to rising the intracellular pH to promote calcification, making the conditions at low-pH sites less favorable for

calcification (de Nooijer *et al.*, 2009). Indeed, this may explain the decrease we see in the total abundance of calcareous porcelaneous and hyaline foraminifera at the low-pH, low-Ω submarine springs.

Agglutinated foraminifera absolute abundance was similar between springs and control sites in three of the five sampled sites, and their relative abundance was similar among springs and controls in four of the five sites (Fig. 2.4), although their abundance was overall low in both springs and control sites. Furthermore, SIMPER analysis revealed that agglutinated *Gaudryina* foraminifera relative abundance increased at low Ω in most of the sites (Fig. 2.3). Since agglutinated foraminifera tests are not made of calcium carbonate, they may be less influenced by the low-Ω seawater at the springs than calcareous foraminifera. A lesser impact of low pH on agglutinated foraminifera abundance has also been observed in foraminifera present at CO_2 vents in Papua New Guinea (Uthicke *et al.*, 2013) and Ischia, in the Mediterranean Sea (Dias *et al.*, 2010). Similarly, the abundance of non-calcifying thecate and agglutinated foraminifera living in direct contact with experimentally injected CO_2 hydrate did not decline significantly with decreasing pH (Bernhard *et al.*, 2009). However, species-specific survival rates of agglutinated foraminifera during a laboratory experiment at 2000 ppm of pCO_2 suggest that other agglutinated species different than *Gaudryina* may respond in a different manner to low Ω (van Dijk *et al.*, 2017).

Since many environmental parameters covary in natural environments (Andersson *et al.*, 2015), including at our field site, it is possible that the trends in

absolute and relative abundances of foraminifera present at the springs are due to species-specific salinity preferences. The salinity of the discharging water at the sampled springs is > 30 for 93% of the time, and it is constantly higher than 27 (Crook *et al.*, 2013). Although the salinity tolerance ranges are not known for all the species found in the study area, many foraminifera that are abundant in shallow warm coastal waters, such as those at our sites, have a very wide salinity tolerance (Brasier, 1980). *Quinqueloculina* spp. has been found at salinity ranges of 12–35 with abundance peaks at 17 and 35 (Horton & Murray, 2007), *Amphistegina lessonii* has been kept at salinities between 25 and 45 in a lab experiment (Geerken *et al.*, 2018), and *Archaias* has been reported to be present at salinities of 29 – 39 (Hallock & Peebles, 1993). Moreover, adaptation to changes in salinity requires increased cellular osmoregulation (McLusky *et al.*, 2004), which is expected to affect both agglutinated and calcareous foraminifera abundance. Since agglutinated foraminifera abundance is similar at the springs and control sites (Fig. 2.4) and does not seem to be affected by the main gradient of variation in carbonate chemistry and salinity (Fig. 2.8), we suggest that Ω and pH are the main drivers of calcareous foraminifera abundances seen in this study. Consistent with this conclusion, the trends we see in the absolute and relative abundance of calcareous and agglutinated foraminifera are in line with observations from other field studies where salinities did not differ between low- and ambient-pH sampling locations (Fabricius *et al.*, 2011; Uthicke *et al.*, 2013). Hence, the lower abundance of calcareous foraminifera we and others have observed in diverse settings with low Ω suggests that a future reduction in Ω will negatively affect calcareous benthic foraminifera.

2.4.2 Relative abundance of foraminifera with porcelaneous, high-magnesium tests increases in low Ω springs

While the absolute abundance of both porcelaneous and hyaline foraminifera was lower at low Ω, a trend towards higher relative abundance of porcelaneous foraminifera and lower relative abundance of hyaline foraminifera is observed (Fig. 2.4). The higher relative abundance of porcelaneous (Fig. 2.4) and high-magnesium foraminifera (Fig. 2.5) is driven by *Archaias angulatus*, which is the most common species found and contributes the most to community dissimilarity in all the sites (Fig. 2.3). *Archaias angulatus* is well preserved in sediments due to its robust, thick test (Hallock & Peebles, 1993), strengthened by crystal pillars (Martin, 1986), and it has been reported to account for more than 20% of the foraminiferal population in the southern Florida shelf (Knorr *et al.*, 2015) and up to 54% of dead assemblages from the northern Florida Keys (Martin, 1986) and is the most common species in Banco Chinchorro in the southern Yucatán Peninsula (Gischler & Möder, 2009). The lower relative abundance of hyaline, low-magnesium foraminifera at low Ω (Figs. 2.4 and 2.5) is attributed to the decrease of *Discorbis* and *Asterigerina* (Fig. 2.3). These results are in contrast with the idea that porcelaneous, high-magnesium foraminifera would be the "first responders" (Fujita *et al.*, 2011) to ocean acidification. This was suggested because high-Mg calcite is more soluble than low-Mg calcite and aragonite at a given pCO_2 (Morse *et al.*, 2006), and because Mg inhibits calcite crystallization.

The calcification pathway of perforate hyaline foraminifera (reviewed by de Nooijer *et al.*, 2014) has been studied in more detail than the calcification process of

porcelaneous foraminifera. Hyaline foraminifera capture ions through seawater endocytosis (Bentov *et al.*, 2009; de Nooijer *et al.*, 2009) and transmembrane transport (Nehrke *et al.*, 2013) and store them in separated intracellular reservoirs of inorganic carbon and calcium (Ter Kuile & Erez, 1991; Toyofuku *et al.*, 2008). A perforated test is then secreted extracellularly within a primary organic sheet after intracellular Mg discrimination and a pH increase in the vacuolated seawater to a pH of ≥ 9 (de Nooijer *et al.*, 2009; Erez, 2003; Zeebe & Sanyal, 2002). In contrast, porcelaneous foraminifera precipitate calcite needles inside intracellular vesicles (at a pH of ~ 9) that are later transported and randomly assembled in an extracellular organic matrix to form a new test chamber (Angell, 1980; de Nooijer *et al.*, 2009; Erez, 2003; Hemleben *et al.*, 1986). These transporting vesicles have been reported to have a pH of 7.5 – 8.0 (de Nooijer *et al.*, 2009). Since these vesicles have a lower pH, it is possible that fewer protons are pumped out of the vesicle. In addition, the lack of internal calcium and inorganic carbon pools may require less energy to precipitate calcite tests, which can be a competitive advantage that explains the increase in relative abundance of porcelaneous foraminifera we see at low-pH, low-Ω springs. Another explanation could be that the lower dissolution rates of the more robust porcelaneous tests (Brasier, 1980; Schmiedl *et al.*, 1997) result in the observed increase in the abundance of these tests. However, further research is needed to test these hypotheses and to better understand the calcification pathway and preservation of porcelaneous foraminifera. These results can guide controlled experiments in a laboratory setting.

2.4.3 Symbiont-bearing foraminifera increase in relative abundance at low Ω springs.

The relative abundance of heterotrophic foraminifera decreased, while the relative abundance of symbiont-bearing foraminifera increased in most of the springs (Fig. 2.6). Foraminifera that host photosynthetic symbionts may be more resilient to low Ω, since they can access additional energy derived from photosynthates translocated from the algae (Hallock, 2000) to increase pH at the calcification site and for alkalinization of seawater vacuoles. In addition, symbiotic algae can promote calcification by removing foraminiferal metabolic N and P, which impede crystal formation, by providing organic matter used to synthesize the organic matrix that precedes test growth (Fujita *et al.*, 2011) and by increasing the pH on the surface of foraminifera (Glas *et al.*, 2012). These mechanisms may explain the significant increase in the relative abundance of symbiont-bearing foraminifera (> 50% of the total calcareous population), while the relative abundance of calcareous heterotrophic foraminifera decreased (< 50 %) at low Ω springs. Although symbiont-bearing calcareous foraminifera were relatively more abundant than symbiont-barren foraminifera at low-Ω sites, their absolute abundance decreased in comparison with sites at ambient Ω, indicating that, despite the symbionts, the conditions were less favorable than at ambient conditions. Short laboratory experiments with symbiont-bearing foraminifera cultured at high pCO_2 have reported reduced net calcification (Fujita *et al.*, 2011; Hikami *et al.*, 2011) and tests dissolution signs (McIntyre-Wressnig *et al.*, 2013). While photosynthetic activity may promote calcification, it did not fully compensate for the deleterious effects of elevated pCO_2 on foraminifera calcification

incubated in laboratory (Glas *et al.*, 2012) and field experiments (Uthicke & Fabricius, 2012). These studies suggest that benthic symbiont-bearing foraminifera can better survive at high pCO_2, but their calcification is reduced.

Foraminifera that host chlorophytes (*Archaias*) were relatively more abundant at springs than those that host diatoms (*Amphistegina* and *Asterigerina*; Fig. 2.7). Hyaline foraminifera that host diatoms were thought to be more resilient to high pCO_2 than other symbiont-bearing foraminifers based on a meta-analysis of studies assessing the impacts of acidification on large benthic foraminifera (Doo *et al.*, 2014). However, none of the studies included in the meta-analyses focused on chlorophyte-bearing foraminifera, and due to the high variability in methodology, duration, and species used in the experiments, it is not possible to make a direct comparison between these studies and an assemblage found at the natural low-Ω springs in our study. Foraminifera that host chlorophytes may be more resilient to ocean acidification than those that host diatoms, or the robustness of *Archaias* tests may be responsible for this difference in relative abundance. It is also plausible that the size of the symbiont-bearing foraminifera influences the survival and preservation under low-Ω conditions. The relative abundance of *Asterigerina* decreased at low Ω while *Amphistegina* increased, in spite of both being hyaline foraminifera that host diatoms (Fig. 2.3). The larger size of *Amphistegina* in comparison to *Asterigerina* may allow for hosting a larger concentration of photosynthetic algae, as it has been suggested that the number of symbionts increases with test size (Hönisch & Hemming, 2004). In fact, *Archaias* has the largest tests of all the species found at the springs in this study. Furthermore, a

larger size has been linked to reduced dissolution due to a smaller surface-to-volume ratio (Hönisch & Hemming, 2004), which may explain why large foraminifera are more abundant overall than smaller foraminifera at this location.

2.4.4 *Discorbis rosea* weight did not significantly vary among springs and control sites

The test weight of *D. rosea* did not significantly vary among springs and control sites. This lack of difference may be due to the large variability in test weight within populations and individuals. The variability in tests weights within a species may be due to differential individual growth rates (Fujita *et al.*, 2011), body sizes (Henehan *et al.*, 2017), or genotypes (Davis *et al.*, 2017) with diverse calcification performance under the same Ω conditions. In our study, the weighted tests were all counted from the 250 –355 μm sediment fraction, and we took special care in selecting individuals of similar size. However, each test was not normalized to shell diameter; hence the wide variability in test weights may be related to the range in test sizes, growth rates or genotypes.

2.4.5 Implications

The reduced absolute abundance of benthic foraminifera at low Ω springs suggest that there may be an overall decrease in benthic foraminifera abundance as a consequence of ocean acidification, with subsequent repercussions on the global carbon cycle and marine food web. *Archaias angulatus*, the most common species found in this study, is known to represent a large proportion of the foraminiferal

population in different parts of the western tropical Atlantic Ocean (Gischler & Möder, 2009; Knorr *et al.*, 2015; Martin, 1986), being the dominant large benthic foraminifera in the Florida – Bahamas carbonate province (Hallock *et al.*, 1986). A laboratory study with *A. angulatus* reported a 50% decrease in growth rate after 28 days at pH 7.6 and an estimated reduction of 85% in carbonate production by this species in the southern Florida Reef Tract and Florida Bay, from 0.27 to 0.04 Mt yr^{-1} (Knorr *et al.*, 2015). Besides changes in carbonate production, a decrease in abundance may have cascade effects on the ecosystem, since foraminifera are an important link in the marine food web, as they prey on bacteria and algae and are predated on by many animals such as gastropods, bivalves, echinoderms, and crustaceans (Culver & Lipps, 2003).

In conclusion, the absolute abundance of large calcareous foraminifera decreased at springs discharging low Ω, low pH water. Porcelaneous, high-magnesium foraminifera were relatively less impacted compared to hyaline foraminifera at the springs, possibly due to their different calcification mechanism, more robust tests, and the lack of internal carbon and calcium pools. The relative abundance of symbiont-bearing foraminifera increased while heterotrophic symbiont-barren foraminifera decreased under low Ω conditions, which may be explained by the higher energy availability provided by the symbiont to elevate the pH at the site of calcification. Chlorophyte-bearing foraminifera were relatively more abundant than diatom-bearing foraminifera. These trends are driven by the abundant large *Archaias angulatus*, porcelaneous foraminifera that host chlorophytes, which may be more resilient to low Ω due to their test's robustness and large size that can lead to a higher concentration of

symbiotic algae and reduced test dissolution. Further laboratory experiments are needed to confirm these results in controlled setting without covarying environmental variables and to better understand the calcification pathway of porcelaneous foraminifera.

2.6 Figures

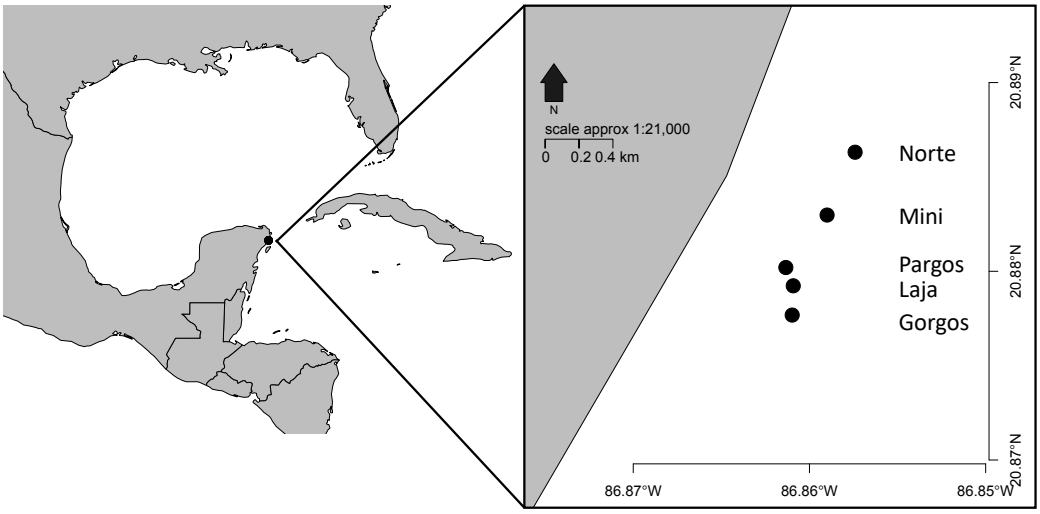

Figure 2.1. Location of low carbonate saturation state submarine springs

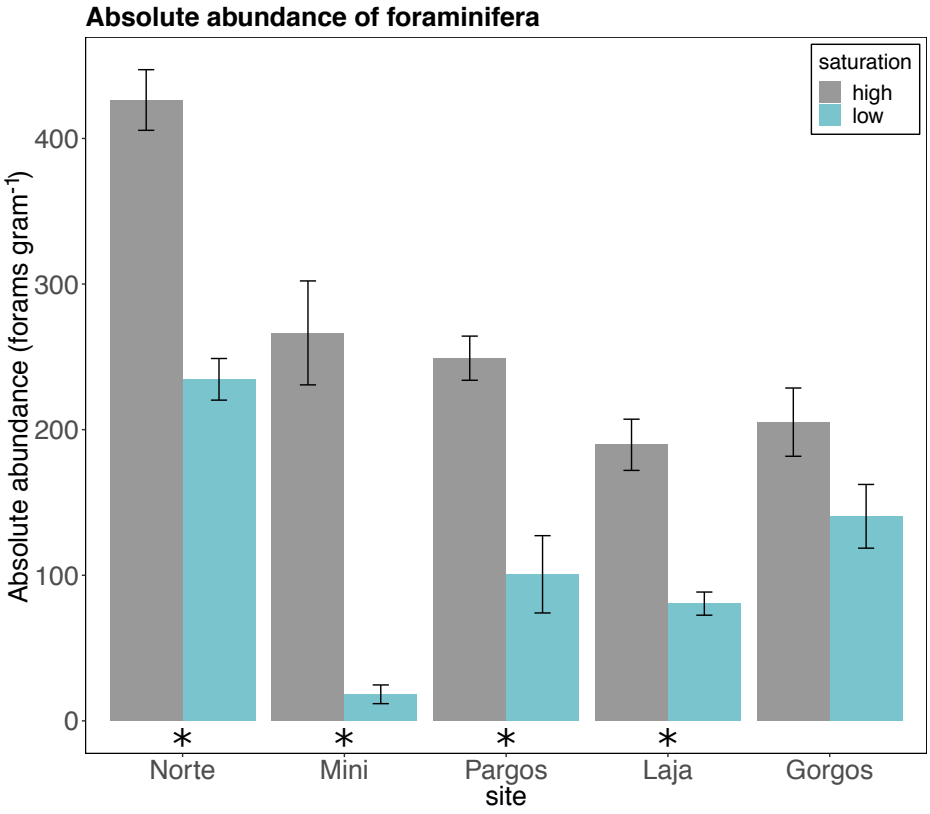

Figure 2.2. Absolute abundance of foraminifera (number of specimens per gram of sediment) in different submarine springs (low saturation state) and their respective control sites (high saturation state). Data are mean ± SE (n= 5). The asterisk demarks a significant difference ($p < 0.05$) in abundance between paired springs and controls at each site according to Mann-Whitney rank sum test.

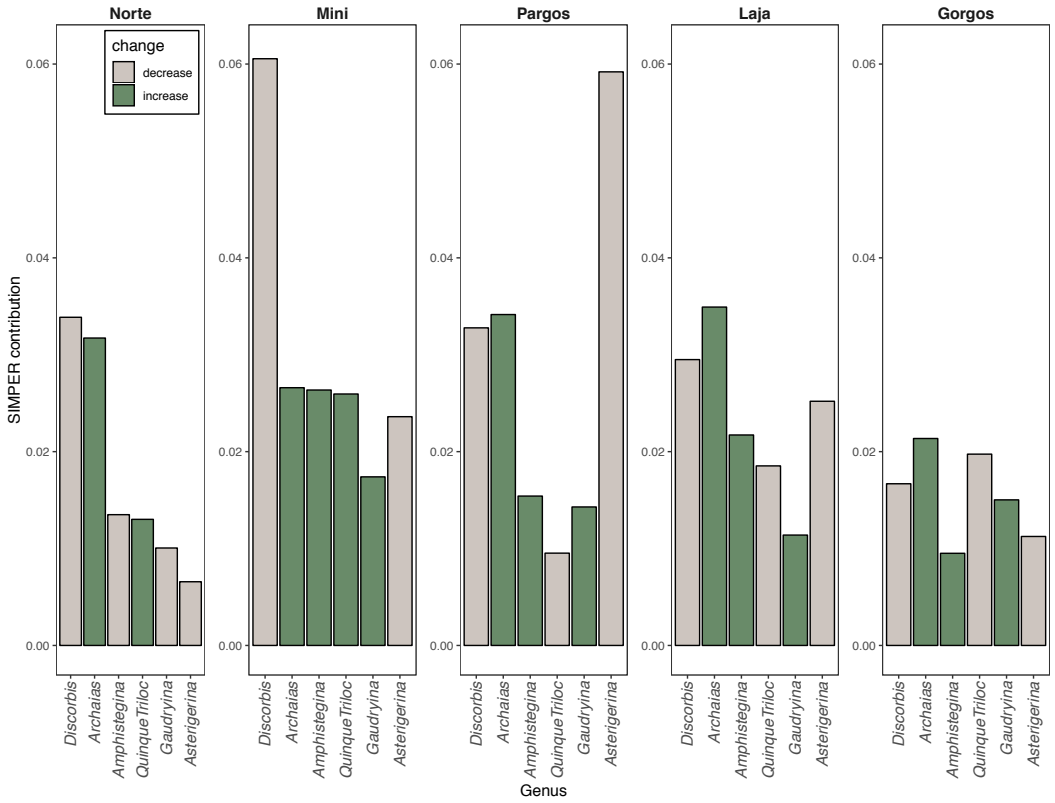

Figure 2.3. SIMPER contribution of the most abundant genera. Bar height indicates the mean contribution of each genus to community dissimilarity. Green color represents an increase and grey color represents a decrease in the mean relative abundance of each genus at low saturation springs.

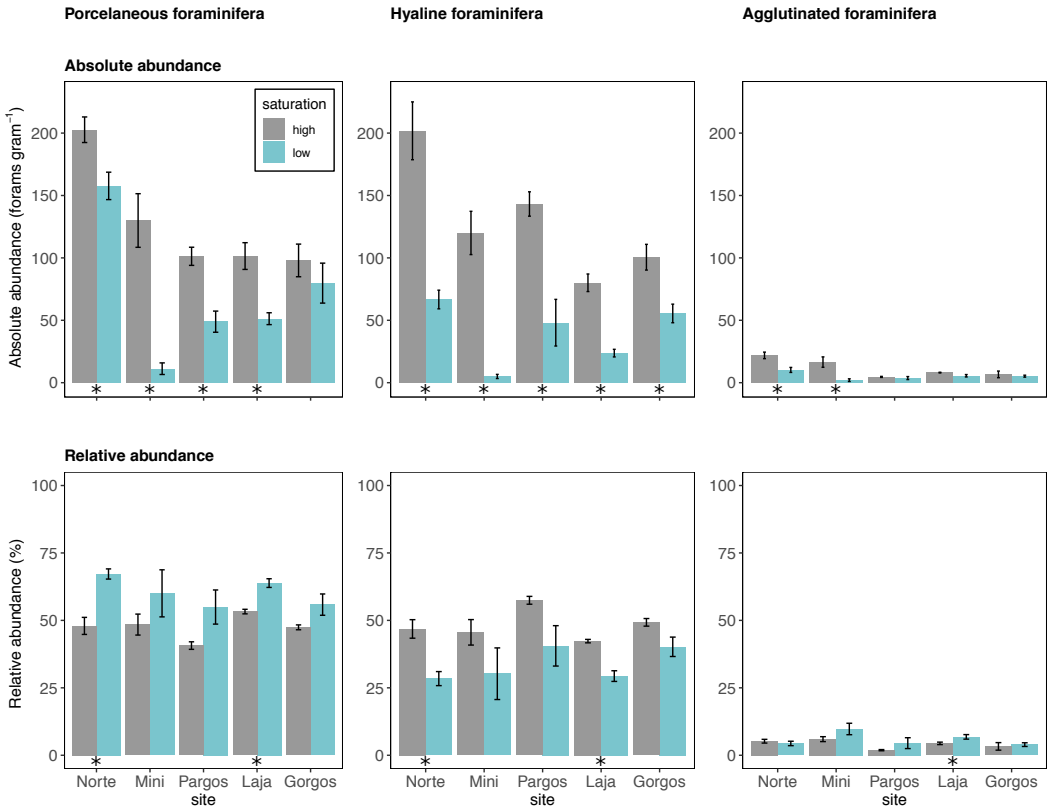

Figure 2.4. Absolute abundance (specimens per gram of sediment) and relative abundance (percentage) of different foraminifera test types (porcelaneous, hyaline, and agglutinated). Data are mean ± SE (n= 5). The asterisk demarks a significant difference ($p < 0.05$) in abundance between paired springs and controls at each site according to Mann-Whitney rank sum test.

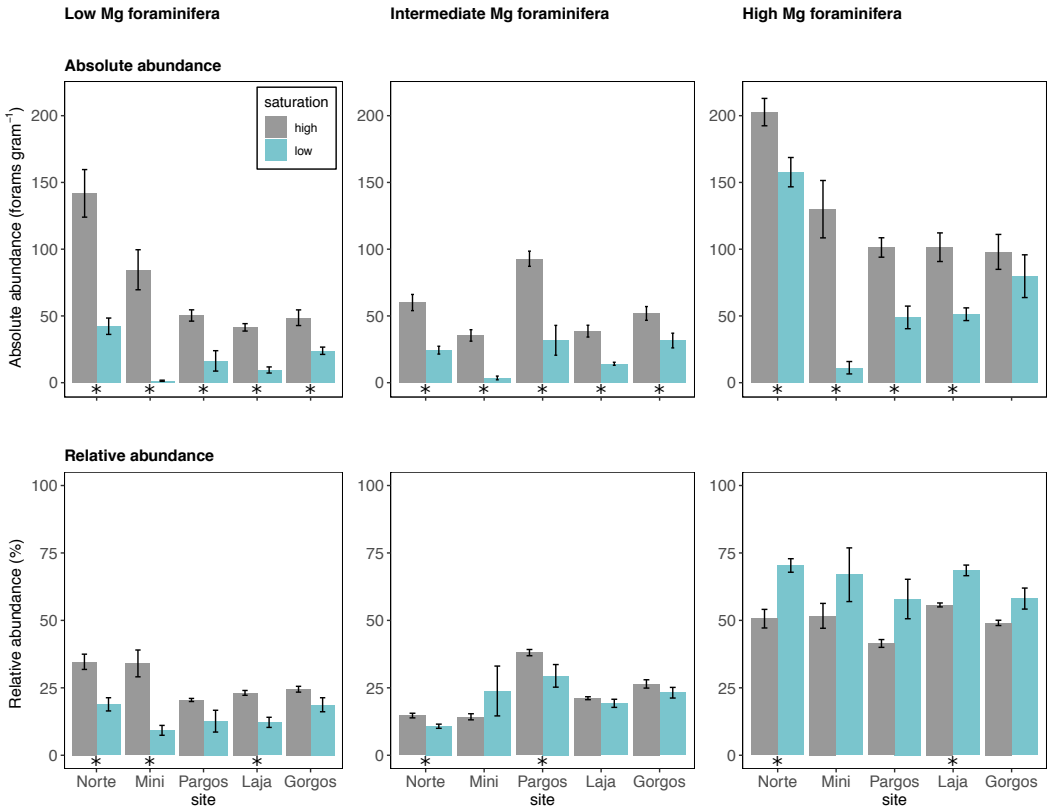

Figure 2.5. Absolute abundance (specimens per gram of sediment) and relative abundance (percentage) of foraminifera with different magnesium content tests. Data are mean ± SE (n= 5). The asterisk demarks a significant difference ($p < 0.05$) in abundance between paired springs and controls at each site according to Mann-Whitney rank sum test.

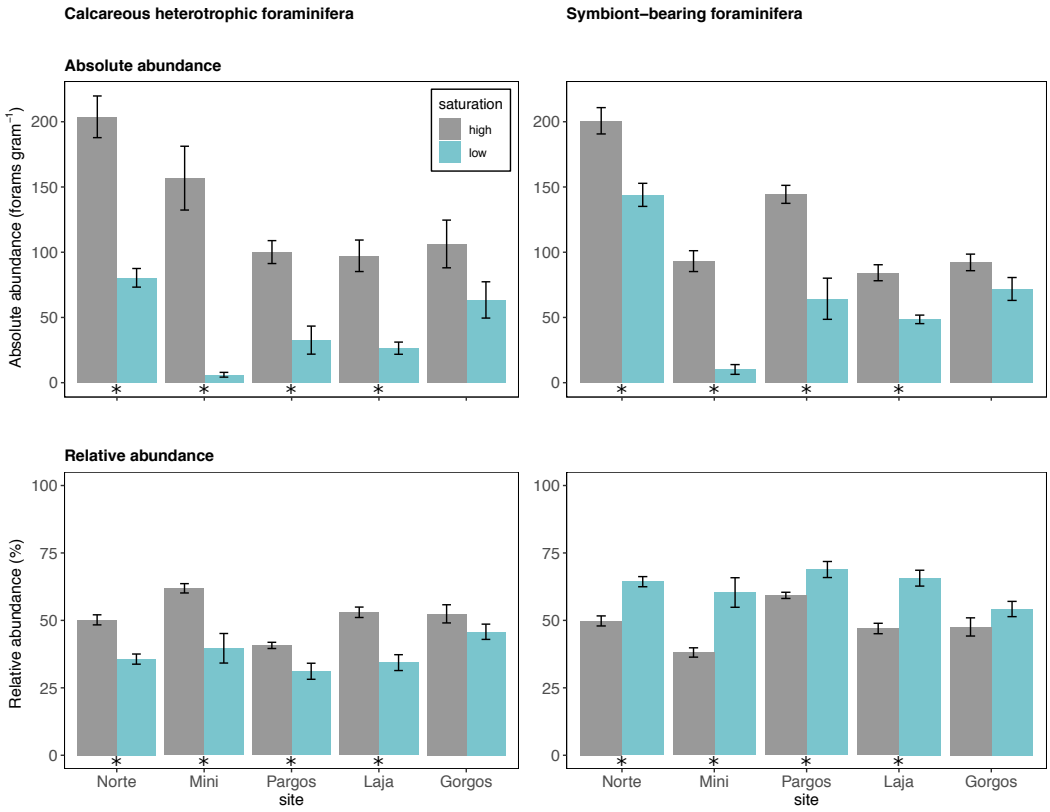

Figure 2.6. Absolute abundance (specimens per gram of sediment) and relative abundance (percentage) of calcareous foraminifera with different feeding strategies (symbiont-barren heterotrophic and symbiont-bearing). Data are mean ± SE (n= 5). The asterisk demarks a significant difference ($p < 0.05$) in abundance between paired springs and controls at each site according to Mann-Whitney rank sum test.

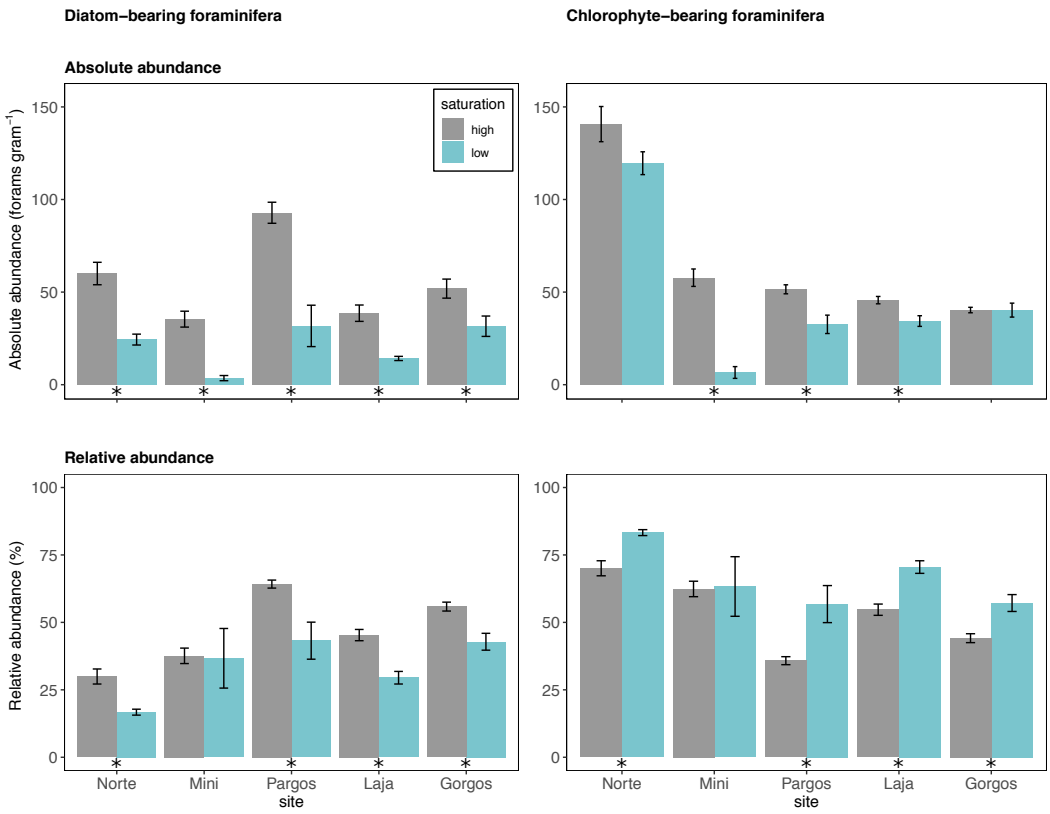

Figure 2.7. Absolute abundance (specimens per gram of sediment) and relative abundance (percentage) of large calcareous foraminifera hosting different symbionts (diatoms and chlorophytes). Data are mean ± SE (n= 5). The asterisk demarks a significant difference ($p < 0.05$) in abundance between paired springs and controls at each site according to Mann-Whitney rank sum test.

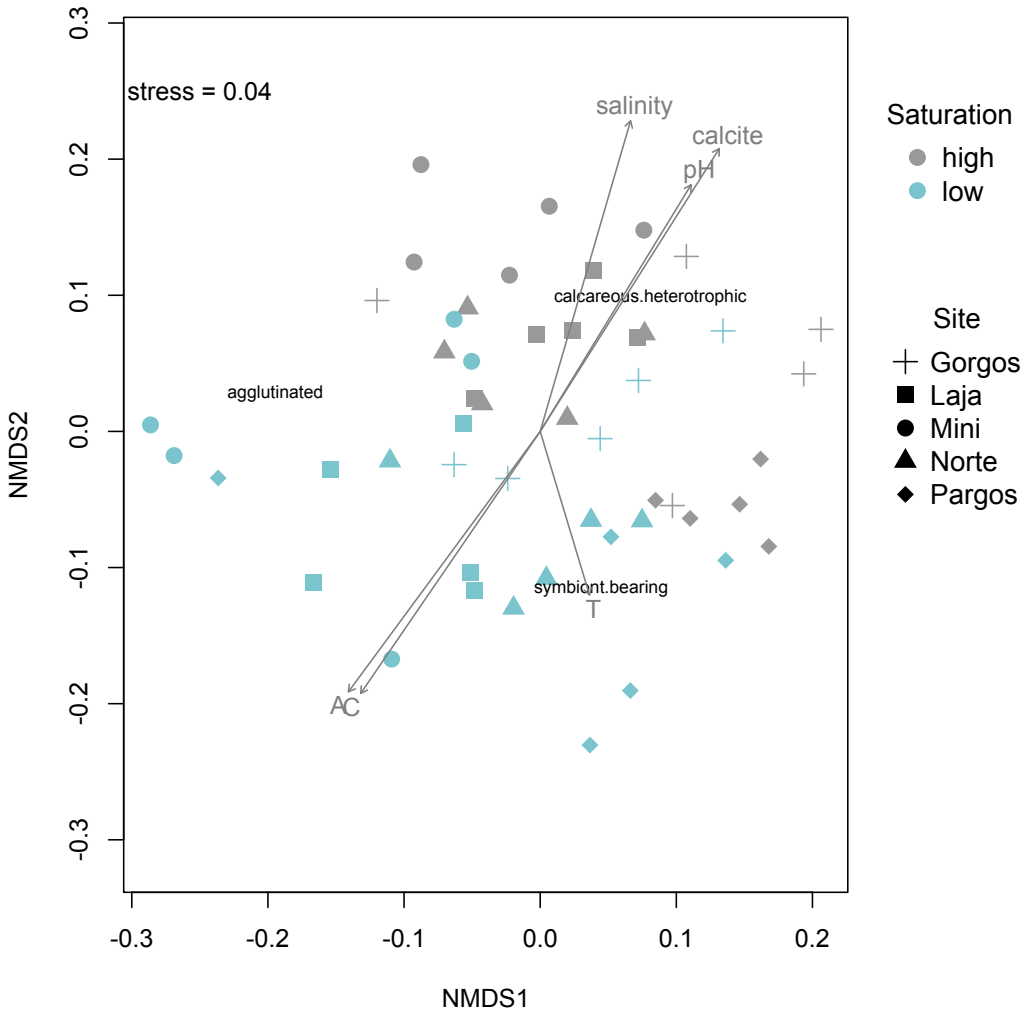

Figure 2.8. Non-metric Multidimensional Scaling (nMDS) ordination plot for community structure (relative abundance) by carbonate saturation state and site with overlaid environmental parameters (A= total alkalinity; C= total inorganic carbon; T= temperature).

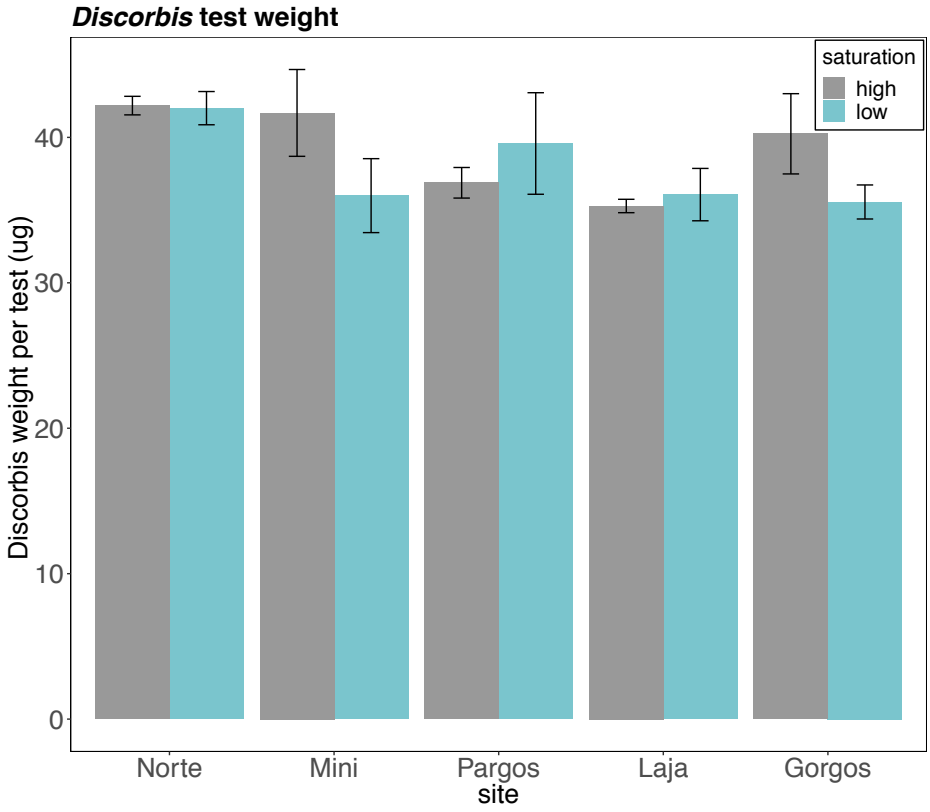

Figure 2.9. Weight of *Discorbis rosea* tests (size fraction 250-355 μm) at low and high saturation at different submarine spring sites. Data are mean ± SE.

2.7 Tables

Table 2.1. Carbonate chemistry parameters of discrete water samples collected at low saturation state submarine springs and adjacent high saturation state control sites (mean ± SD) at the time of sample collection (A_T= total alkalinity; C_T= total inorganic carbon). * Calculated using CO_2Sys

Site	Depth (m)		A_T (µmol·kg^{-1})	C_T (µmol·kg^{-1})	*pH	*CO_3^{2-} (µmol·kg^{-1})	*$\Omega_{calcite}$	T (°C)	Salinity
Norte	5.8	control	2354 ± 13	2051 ± 6	7.98	216.16	5.14	27.0	36.80
		spring	2611 ± 3	2588 ± 3	7.38	67.03	1.66	27.5	32.21
Mini	4.9	control	2356 ± 3	2049 ± 6	7.99	218.13	5.16	26.4	37.3
		spring	3108 ± 10	3197 ± 6	7.13	46.29	1.14	27.6	32.41
Pargos	6.8	control	2336 ± 4	2012 ± 12	8.01	229.56	5.49	27.6	36.17
		spring	3000 ± 8	3048 ± 12	7.23	52.73	1.33	27.6	29.95
Laja	5.8	control	2357 ± 6	2092 ± 1	7.90	193.55	4.63	28.1	36.17
		spring	2827 ± 9	2756 ± 10	7.51	102.65	2.50	27.9	32.75
Gorgos	7.2	control	2325 ± 3	2033 ± 3	7.96	209.44	5.02	27.8	35.90
		spring	2874 ± 11	2987 ± 8	7.11	94.65	2.38	28.5	31.09

Chapter 3. Phenotypic variability of Caribbean corals' calcification after two-year transplantation to low aragonite saturation submarine springs

Ana Martinez[1], Elizabeth D. Crook[2], Daniel J. Barshis[3], Donald C. Potts[4], Mario Rebolledo-Vieyra[5], Laura Hernandez[6] and Adina Paytan[7]

[1] Department of Earth and Planetary Science, University of California Santa Cruz, Santa Cruz, California, USA

[2] Department of Earth System Science, University of California Irvine, Irvine, California, USA

[3] Department of Biological Sciences, Old Dominion University, Norfolk, Virginia, USA

[4] Department of Ecology and Evolutionary Biology, University of California Santa Cruz, Santa Cruz, California, USA

[5] Chipre 5, Resid. Isla Azul, Cancún, Quintana Roo, 77500, México

[6] Universidad del Caribe, L-1. Mz 1, Esq. Fracc. Tabachines SM 78, Cancún, Quintana Roo, 77528, México

[7] Institute of Marine Sciences, University of California Santa Cruz, Santa Cruz, California, USA

Abstract

Coral calcification is expected to decline as atmospheric carbon dioxide concentration increases. We assessed the potential of corals to survive and calcify under acidified conditions in a two-year field transplant experiment around low pH, low aragonite saturation (Ω_{arag}) submarine springs along the Mexican Caribbean coast. We used three common Caribbean corals: the massive *Porites astreoides* and *Siderastrea siderea,* which live naturally in proximity to the springs, and the branching *Porites porites,* which is absent near springs. Fragments were collected from coral colonies living at low pH-low Ω_{arag} springs and from colonies living at ambient pH and Ω_{arag} conditions in the lagoon (*P. astreoides n=40* and *S. siderea n=38*) as well as from colonies living at the adjacent reef (*S. siderea n=20, P. porites n=20*). Fragments from each colony were transplanted to a low Ω_{arag} spring and an ambient Ω_{arag} control site. Slow-growing *S. siderea* had the highest post-transplantation survival and increased tissue concentrations of Symbiodiniaceae, chlorophyll *a*, and protein in the low Ω_{arag} site. Nubbins of *P. astreoides* had 20% lower survival and higher chlorophyll *a* concentration at the low Ω_{arag} site. Only 33% of *P. porites* nubbins survived at low Ω_{arag} and their linear extension and calcification rates were reduced. The density of skeletons deposited after transplantation was 15-30% lower for all species at the low Ω_{arag} spring vs. the control site. These results suggest that corals with slow calcification rates and high Symbiodiniaceae, chlorophyll *a* and protein concentrations may be less susceptible to ocean acidification, albeit with reduced skeletal density. We postulate that corals in the springs are responding to greater energy demands for overcoming

larger differences in carbonate chemistry between the calcifying medium and the external environment. The differential mortality, growth rates and physiological changes may impact future coral species assemblage and the reef framework robustness.

3.1 Introduction

Anthropogenic activities are increasing the amount of carbon dioxide entering the atmosphere. A large fraction of this CO_2 dissolves in the ocean and lowers ocean pH and carbonate ion concentrations (Kleypas *et al.*, 1999) in a process called ocean acidification (Caldeira & Wickett, 2003). Low carbonate ion concentrations decrease the aragonite saturation state (Ω_{arag}) of seawater and the availability of carbonate ions needed for deposition of calcium carbonate skeletons (Smith & Buddemeier, 1992). A meta-analysis of experimental studies found a decrease of ~15% in coral calcification rates per unit decrease in Ω_{arag} (Chan & Connolly, 2013). Data from laboratory experiments and modeling suggest that coral reef carbonate accretion diminishes at Ω_{arag} lower than 3.3 (Hoegh-Guldberg *et al.*, 2007), a level likely to be reached in much of the surface ocean by 2100 (Gattuso *et al.*, 1999; Kleypas *et al.*, 1999). Many laboratory experiments have reported reduced coral growth under low Ω_{arag} (e.g., de Putron *et al.*, 2011; Gattuso *et al.*, 1998; Krief *et al.*, 2010), but other experiments show little impact on calcification (Comeau *et al.*, 2013; Edmunds *et al.*, 2012; Jury *et al.*, 2010; Reynaud *et al.*, 2003; Ries *et al.*, 2009; Rodolfo-Metalpa *et al.*, 2010). These conflicting results reflect the limitations of short-term single-organism manipulative

experiments since, while laboratory experiments allow precise control of physicochemical parameters, they do not fully reflect the complexity of the natural environment (Andersson, 2015). Moreover, such experiments are often too short for organisms to fully acclimate (Form & Riebesell, 2012).

Scleractinian corals have been observed living in low pH waters near CO_2 vents (pH < 7.7; Fabricius *et al.*, 2011) and low Ω_{arag} submarine springs (Ω_{arag} <1; Crook *et al.*, 2012), although the taxonomic richness at these sites is lower than at nearby sites with ambient carbonate chemistry. At high CO_2 vents in the Mediterranean, temperate corals were absent at Ω_{arag} < 2.5 (Hall-Spencer *et al.*, 2008), although two species that were transplanted to these low pH vents survived and grew at species-specific calcification rates (Rodolfo-Metalpa *et al.*, 2011). While these studies indicate that some temperate corals can calcify under relatively low Ω_{arag} conditions, it is not known if tropical corals transplanted to low Ω_{arag} seawater sites can survive, acclimatize and persist under continuous ocean acidification conditions. We investigated the survival, physiological response, and calcification rate of three species of Caribbean corals in a 2-year long, *in-situ* transplantation experiment leveraging naturally-occurring low pH, low Ω_{arag} submarine springs.

Off the Yucatan peninsula, Mexico, submarine groundwater springs discharge low pH, low Ω_{arag} water (Ω_{arag} ~ 0.5) into the lagoon of the Mesoamerican Barrier Reef. These springs, locally referred to as “ojos”, can be used for testing the potential of

corals to acclimatize or adapt to future low Ω_{arag} conditions. The groundwater mixes with seawater before discharging (Back *et al.*, 1979), and sensor and discrete sampling data demonstrate that the discharged water has relatively high dissolved inorganic carbon, high alkalinity and slightly lower than ambient salinity in addition to the low pH and low Ω_{arag} (Crook *et al.*, 2012; Crook *et al.*, 2013; Crook *et al.*, 2016; Hofmann *et al.*, 2011; Null *et al.*, 2014; Paytan *et al.*, 2014). Only three scleractinian coral species (*Siderastrea siderea, Porites astreoides*, and *Porites divaricata*) grow within the areas continuously exposed to low Ω_{arag} conditions at the ojos, but taxonomic richness increases away from the discharge sites (Crook *et al.*, 2012). Coral colonies living in the low Ω_{arag} seawater are smaller than those exposed to ambient seawater (Crook *et al.*, 2012) and have lower skeleton densities and calcification rates (Crook *et al.*, 2013).

We assessed the potential of three coral species to survive and calcify under low Ω_{arag} conditions by conducting an *in-situ*, transplant experiment with genetically identical coral fragments (nubbins) in the lagoon close to the ojos. We monitored the corals for two years and collected surviving nubbins for analyses of skeletal characteristics (density, linear extension, calcification rate), and physiological characteristics (coral tissue protein content, and cell densities and chlorophyll *a* concentration of photosymbiotic algae Symbiodiniaceae). We then compared coral responses among transplantation sites to determine their acclimation potential to low Ω_{arag}. We also examined differences among nubbins collected from distinct origins to

elucidate putative genotypic influences that may allow coral populations to survive and calcify at ocean acidification conditions.

3.2 Materials and methods

3.2.1 Study area

The Yucatan peninsula, Mexico, is a karstic region where rainfall percolates rapidly through the ground and flows through a complex aquifer system that discharges low pH, low Ω_{arag} water through fractures as submarine springs (ojos) in the lagoon between the Mesoamerican barrier reef and the mainland (Back & Hanshaw, 1970). The submarine ojos are surrounded by seagrass meadows and discharge ~500 m from the coast and ~1 km from the barrier reef in a water depth of ~6 m. While these ojos occur along the entire karst platform and have been discharging since the rise in sea level associated with the retreating ice sheets after the last glacial maximum (Beddows *et al.*, 2002), approximately 13 individual ojos have been closely monitored near the coast of Puerto Morelos since 2008. Therefore, the Puerto Morelos coast was chosen for this particular study (20.8° N, 86.8° W).

3.2.2 Coral species and transplant experiment design

We collected two genetically identical fragments (nubbins) each from 20 *Porites astreoides* colonies and 19 *Siderastrea siderea* colonies from areas in close proximity to the ojo discharge (20 colonies), and from adjacent control sites away from the influence of discharge (19 colonies) (see Table 3.1 for collection details). Both species are found throughout the lagoon, including within low Ω_{arag} ojo discharge

plumes (Crook *et al.*, 2012). We also collected two nubbins each from 10 *Porites porites* colonies, a species not found in the lagoon, and from 10 additional *S. siderea* colonies from the main barrier reef structure. From each genotype/colony, one nubbin was transplanted to a low Ω_{arag} site (ojo) and the second was transplanted to an ambient Ω_{arag} site (control) in the lagoon, ~5 meters away from the discharge site. A total of 59 colonies and 118 nubbins were transplanted to the two sites (see Table 3.2 for transplantation details and Fig. 3.1 for transplant experiment design). One nubbin of *P. porites* transplanted to low Ω_{arag} ojo was lost in the process and was not included in further analyses.

Nubbins of approximately 2-3 cm in length of massive *P. astreoides* and *S. siderea* were extracted by coring with a submersible pneumatic drill with a 3 cm diameter drill bit. After coring, the remaining coral colony was patched with epoxy putty to prevent bioerosion and provide a surface for regrowth. *P. porites* nubbins were small branches (~3-5 cm long) broken off each colony with pliers. Each nubbin was mounted on a 5 x 5 cm square of stainless-steel mesh (6 mm) with epoxy putty that also covered all exposed skeletal surfaces to prevent bioerosion. Each nubbin was individually labeled with a stainless steel or plastic tag tied to the mesh. The nubbins were placed in shallow trays with seawater and alizarin red dye for 6 - 8 hours to stain the surface and mark the beginning of new skeleton growth (Barnes, 1970). After staining, each nubbin was photographed, and then nubbins were randomly assigned to one of the transplantation sites (low Ω_{arag} ojo or ambient Ω_{arag} control). Within transplant sites, nubbins were randomly assigned to positions on stainless steel grids

(24 mm mesh) and attached to the grids with cable ties (Fig. 3.2). At the low Ω_{arag} site, the grids were attached with cable ties to stainless steel lag screws drilled into exposed rock as close as possible to the maximum discharge point. Control grids were cable-tied to concrete blocks placed within the seagrass beds on the lagoon seafloor.

Divers monitored the nubbins weekly for the first two months and then 14 times for the following 22 months. Monitoring included obtaining water samples and photographing each nubbin and taking notes on condition and mortality. At the end of the transplant experiment, all surviving nubbins were collected and preserved in liquid nitrogen.

3.2.3 Water chemistry

Water samples were collected weekly for the first two months of the experiment and then 7 times for the following 22 months of the transplantation experiment at the ojo (n = 17) and control sites (n = 15). Water samples were collected by divers using acid-washed, sample-rinsed syringes and injected into HDPE bottles. Temperature was measured with a handheld probe (YSI model 63) and water samples were filtered (0.2 μm) into glass bottles and preserved with saturated mercuric chloride solution following procedures of Dickson *et al.* (2007). Total inorganic carbon was measured with a CM5011 Carbon Coulometer (UIC, Inc). Alkalinity was measured with an automated open-cell, potentiometric titrator (Orion model 950). Salinity was measured with a salinometer (Portasal Model 8410, Guild Line). Certified CO_2 seawater standards (from A. Dickson lab UC San Diego # 108 and 135) were used as reference

material. Aragonite saturation state (Ω_{arag}) was calculated using the CO_2Sys program (Pierrot *et al.*, 2006) with constants from Mehrbach *et al.* (1973) refit by Dickson and Millero (1987). All seawater chemistry analyses were performed in the Marine Analytical Laboratory of the Institute of Marine Science at the University of California, Santa Cruz.

3.2.4 Tissue extraction and skeletal analysis

Coral tissues were extracted from the frozen coral samples with an airbrush using artificial seawater. Aliquots of the homogenized tissue were used for protein, symbiont cells and chlorophyll *a* measurements following the procedures of Krief *et al.* (2010). Coral skeletons were then submerged in 10% sodium hypochlorite overnight to remove remnant tissue. Each nubbin was sliced vertically with a diamond rock saw through the primary growth axis. Linear extension of new skeleton above the alizarin red mark was measured to the nearest millimeter under a microscope with graduated lenses. A piece (surface area: ~2 cm^2) of coral skeleton deposited after transplanting was cut from the top of the alizarin red mark to the top of the coral, and its enclosed volume was calculated following the procedure of Smith *et al.* (2007) to determine the bulk density of skeleton deposited after transplantation using the buoyant weight method (Davies, 1989; Jokiel & Maragos, 1978). The annual calcification rate (g cm^{-2} $year^{-1}$) was calculated as the product of linear extension (cm $year^{-1}$) and density (g cm^{-3}).

3.2.5 Tissue analysis

Symbiodiniaceae (LaJeunesse *et al.*, 2018) concentrations were determined in triplicate with a hemocytometer and symbiont counts were normalized to skeleton surface area (Symbiodiniaceae cell cm^{-2}). Surface area was calculated with a standard curve created using the paraffin wax method (Stimson & Kinzie III, 1991). Chlorophyll *a* was extracted in 90% acetone and concentration was measured with a spectrophotometer (Genesys 10s UV-VIS, ThermoScientific), calculated with equations in Jeffrey & Humphrey (1975), and the chlorophyll *a* concentrations were then divided by Symbiodiniaceae cell concentrations (μg Symbiodiniaceae $cell^{-1}$). Protein concentration was determined with a Nanodrop 2000 spectrophotometer and then divided by skeleton surface area (mg cm^{-2}).

3.2.6 Statistical analysis

Statistical analyses were performed with R version 3.4.3 (Team, 2015) and plots were made with the "ggplot2" package in R (Wickham, 2016). The "survival" package (Therneau & Lumley, 2015) was used to plot Kaplan-Meier survival curves and Mantel-Cox Log Rank tests were used for statistical comparisons among survival curves. Mann-Whitney U non-parametric tests were used when comparing two groups (i.e., transplantation sites) and Kruskal-Wallis non-parametric tests for comparing three groups (i.e., coral species and coral origins) followed by Pairwise Mann-Whitney U post-hoc tests. Non-parametric tests were used due to the effect of differential sample size on heterogeneity of variances.

3.3 Results

3.3.1 Water chemistry

The total alkalinity and dissolved inorganic carbon of water samples collected during the two-year transplant experiment were higher at ojo than at control transplantation site (total alkalinity: Mann-Whitney U, $W = 244$, $p < 0.001$; dissolved inorganic carbon: $W = 252$, $p < 0.001$) (Table 3.3). Average total alkalinity was 2759 μmol kg^{-1} at the ojo site and 2365 μmol kg^{-1} at the control site and average dissolved inorganic carbon was 2621 μmol kg^{-1} at the ojo and 2019 μmol kg^{-1} at the control site. The salinity and the calculated Ω_{arag} and pH were lower at the ojo vs. the control transplantation site (salinity: $W = 6$, $p < 0.001$; Ω_{arag}: $W = 32$, $p < 0.01$; pH: $W = 50$, $p < 0.01$). The average salinity, Ω_{arag} and pH were 33.3, 2.10 and 7.70 respectively at the ojo transplantation site and 35.6, 3.53 and 8.17 at the control transplantation site. Temperature fluctuated throughout experiment but did not differ among transplantation sites (~27°C ± 0.3 SE; $W = 122$, $p = 0.676$).

3.3.2 Survival

Two years after transplantation, the survival of *P. astreoides* nubbins transplanted to the ojo was lower (60%) than those transplanted to the control site (90%) (Log rank test: $\chi^2 = 4.1$, $df = 1$, $p = 0.042$; Fig. 3.3). The survival of *P. astreoides* nubbins originating from ojos was qualitatively lower (65%) than those originated from control sites (85%), although the survival curves did not differ ($\chi^2 = 2.2$, $df = 1$, $p = 0.141$). *S. siderea* survival was similar among transplantation sites (control: 96%; ojo: 86.2%; Log rank test: $\chi^2 = 2$, $df = 1$, $p = 0.16$), but survival of nubbins originating from

the reef was marginally lower (80%) than those originating from ojos (100%) and controls (94.4%) (χ^2 = 5.6, df = 2, p = 0.062). All *P. porites* nubbins originated from the reef, and their survival at the ojo transplantation site was marginally lower (33.3%) than those at the control site (80%), but their survival curves were not different (χ^2 = 2.9, df = 1, p = 0.087).

3.3.3 Density

At the end of the experiment, the skeletal density of corals transplanted to the ojo was lower than that of corals transplanted to the control site for all three species (Fig. 3.4). The median density of coral skeletons transplanted to ojo and control sites, respectively, was 1.10 g cm^{-3} ± 0.03 SE and 1.58 g cm^{-3} ± 0.02 SE for *P. astreoides*, (Mann-Whitney U: W = 150, p < 0.001); 1.38 g cm^{-3} ± 0.03 SE and 1.63 g cm^{-3} ± 0.02 SE for *S. siderea* (W = 250, p < 0.001); and 1.29 g cm^{-3} ± 0.07 SE and 1.72 g cm^{-3} ± 0.05 SE for *P. porites* (W =20, p = 0.033). Skeletal density of *P. astreoides* originating from ojos and control sites was similar (W = 85, p = 0.728). Skeletal density of *S. siderea* differed based on nubbin origin (Kruskal-Wallis: H = 7.783, df = 2, p = 0.020). Density of *S. siderea* nubbins originating from ojos was lower than that of nubbins originating from the reef (p = 0.017) but was not different than nubbins originating from control sites (p = 0.163). Density of *S. siderea* nubbins originating from control sites and from the reef did not differ (p = 0.508).

3.3.4 Linear extension

After two years of experimentation, linear extension of *P. astreoides* did not vary among transplantation sites (Mann-Whitney U: W = 59.5, p = 0.079) or origins (W = 77, p = 0.245; Fig. 3.4). *S. siderea* linear extension did not vary among transplantation sites (W = 257, p = 0.302) but it varied based on nubbin origin (Kruskal-Wallis: H = 16.679, df = 2, p < 0.001). Linear extension of *S. siderea* nubbins originating from the reef was higher (0.31 cm $year^{-1}$) than nubbins originating either from control (0.19 cm $year^{-1}$, p = 0.004) or ojo sites (0.16 cm $year^{-1}$, p < 0.001). Linear extension of *P. porites* nubbins transplanted to the ojo was half of that of nubbins transplanted to control site (W = 21, p = 0.017).

3.3.5 Calcification

P. astreoides calcification did not differ among transplantation sites (Mann-Whitney U: W = 72, p = 0.815) or origins (W = 46, p = 0.143; Fig. 3.4). Calcification rates of *S. siderea* also did not vary with transplantation site (W = 144, p = 0.762), but they did differ with nubbin origin (Kruskal-Wallis: H = 15.113, df = 2, p < 0.001). Calcification of *S. siderea* nubbins originated from the reef was almost double than those from ojo sites (p < 0.001), and 36% more than nubbins originated from control sites (p = 0.058). The calcification rate of *P. porites* was ~66% lower at ojo than at control transplantation site (W = 21, p = 0.017).

3.3.6 Symbiodiniaceae concentration

Symbiodiniaceae concentration per surface area of *S. siderea* was higher at the ojo (median: 1.26 x 10^7 cell cm^{-2}) vs. the control transplantation site (2.50 x 10^6 cell cm^{-2}, Mann-Whitney U: W = 75, $p < 0.001$; Fig. 3.5). Concentration did not differ among transplantation sites for either *P. astreoides* (W = 52, p = 0.183) or P. *porites* (W = 4, p = 0.857). No coral species differed in Symbiodiniaceae concentration based on collection origin (*P. astreoides*: W = 73, p = 0.81; *S. siderea*: Kruskal-Wallis, H = 2.469, df = 2, p = 0.291).

3.3.7 Chlorophyll *a* concentration

Chlorophyll *a* concentrations per Symbiodiniaceae (μg/ Symbiodiniaceae cell) of both *P. astreoides* and *S. siderea* were higher at the ojo vs. the control transplantation site (*P. astreoides*: Mann-Whitney U, W = 15, $p < 0.001$; *S. siderea*: W = 57.5, $p < 0.001$; Fig. 3.5). Chlorophyll *a* concentration per Symbiodiniaceae of *P. astreoides* and *S. siderea* did not differ based on origins (*P. astreoides*: W = 98, p = 0.719; *S. siderea*: Kruskal-Wallis, H = 4.151, df = 2, p = 0.125). Chlorophyll *a* concentration per Symbiodiniaceae of *P. porites* did not differ among transplantation sites (W = 4, p = 0.262).

3.3.8 Protein concentration

The protein concentration (mg cm^{-2}) of *S. siderea* nubbins transplanted to the ojo was twice that of nubbins transplanted to the control (Mann-Whitney U: W = 119, p = 0.006; Fig. 3.5), but there were no differences among transplantation sites for either

P. astreoides (W = 75, p = 0.936) or *P. porites* (W = 7, p = 0.571). Protein concentration did not differ among nubbin origins for *P. astreoides* (W = 98, p = 0.267) or *S. siderea* (Kruskal-Wallis, H = 4.807, df = 2, p = 0.090).

3.4 Discussion

This study demonstrated that after two years of *in-situ* transplantation, three Caribbean coral species (*Porites astreoides*, *Porites porites* and *Siderastrea siderea*) were able to survive and calcify at low Ω_{arag} seawater, however, their skeletal density decreased while net linear extension and calcification rates were maintained. *S. siderea* nubbins had the highest survival and responded to low Ω_{arag} by increasing the concentration of Symbiodiniaceae, chlorophyll *a* and protein.

3.4.1 Survival of slow-growing corals was higher than fast-growing corals transplanted to low Ω_{arag}

The survival of slow-growing massive *P. astreoides* and *S. siderea* was higher at low Ω_{arag} than faster-growing branching *P. porites* (Fig. 3.3), indicating a species-specific tolerance to ocean acidification. This is consistent with the coral assemblages naturally found at our study site: massive colonies of *P. astreoides* and *Siderastrea* are abundant at low Ω_{arag} ojos, the branching *P. divaricata* is present in very low numbers, and branching *P. porites* is absent (Crook *et al.*, 2012). Similarly, massive *Porites* corals were twice as abundant, while the abundance of structurally complex (e.g., branching) corals was a third lower at high pCO_2 volcanic seeps than at ambient Ω_{arag}

sites in Papua New Guinea (Fabricius *et al.*, 2011), and massive Pavonid corals were least sensitive to acidification in Pacific Panama (Manzello, 2010). While these results suggest massive corals have an advantage over branching corals at low Ω_{arag} sites, it may be attributed to differential growth rates rather than morphologies, since morphology was found to be unrelated to calcification of corals experimentally incubated at high pCO_2 (Comeau *et al.*, 2014; Lenz & Edmunds, 2017) . Fast growing corals may be more affected by low Ω_{arag} because their rapid calcification makes them more sensitive to low carbonate ion availability (Rodolfo-Metalpa *et al.*, 2010) and requires them to remove protons from the calcification site fast enough to maintain an adequate inner pH (Comeau *et al.*, 2014), with a concomitant increased energy demand.

3.4.2 Skeletal density was lower at low Ω_{arag} transplantation site

While calcification rates (density x linear extension) were not consistently lower at ojo transplantation site, the skeletal density was 15 - 30% lower. This suggests these corals maintained their linear extension at the expense of density (Fig. 3.4). Linear extension is inversely correlated with density because faster extension rate result in less time for skeleton thickening (Lough & Barnes, 2000). Similar density and porosity differences occur naturally in *P. astreoides* sampled at ojos and control sites and measured with computerized tomography (Crook *et al.*, 2013) . This suggests that the differences in our study were not artifacts of the transplantation process, and that corals experiencing low Ω_{arag} conditions for their entire lives do not achieve the skeletal densities as their counterparts in ambient Ω_{arag} water. Our data show that when moved

to a more favorable environment, the corals can acclimatize and increase their skeletal density.

Phenotypically plastic skeletons have been described in many corals under a variety of environmental factors, with high density skeletons associated with high Ω_{arag} (Mollica *et al.*, 2018), high temperature (Highsmith, 1979), low cloud coverage and rainfall (Lough & Barnes, 1989), low turbidity and sediment load (Carricart-Ganivet & Merino, 2001), and high hydraulic energy (Smith *et al.*, 2007). In field studies, several environmental variables often covary and isolating the effect of a single environmental factor is challenging. In our experiment, most parameters except carbonate chemistry were very similar at both transplantation sites, which emphasizes the role of low Ω_{arag} in reducing density in this specific case. Field and laboratory studies collectively indicate that coral growth at low Ω_{arag} waters usually results in precipitation of lower density skeletons (Crook *et al*., 2013; Fantazzini *et al.*, 2015; Mollica *et al*., 2018; Tambutté *et al*., 2015). Decoupling extension and density, and the processes that control each, will increase our understanding of coral calcification and potential acclimation in low Ω_{arag} waters. Neither calcification rate nor skeletal growth alone fully reflect the effects of low Ω_{arag} on coral skeleton health; it is necessary to take into consideration three aspects of coral growth (density, linear extension and calcification rate) as done in our and other studies (Fantazzini *et al.*, 2015) to avoid conflicting results on the effects of ocean acidification on calcification.

Although all the *S. siderea* nubbins originating from the ojos survived the 2-year transplantation experiment, their skeletal density, linear extension and calcification rates were lower than that of nubbins originating from the reef site. It is possible that the early life history of corals is affected by low pH (Albright, 2011), impacting their ability to respond to changing conditions later in life or that the populations have been physically isolated for extended time allowing some genetic divergence.

3.4.3 Concentrations of Symbiodiniaceae, chlorophyll *a* and proteins were higher at low Ω_{arag} ojo transplantation site

The higher concentrations of Symbiodiniaceae, chlorophyll *a* and tissue protein of *S. siderea* nubbins transplanted to the ojo (Fig. 3.5) may be responsible for *S. siderea's* ability to survive and calcify at low Ω conditions. Calcification requires transport of inorganic carbonate and calcium ions to the calcifying medium. Calcium carbonate precipitation produces protons that must be removed from the extracellular calcifying medium by Ca^{2+}-ATPase to maintain a high Ω_{arag} (Al-Horani *et al.*, 2003; Allemand *et al.*, 2011; Cohen & McConnaughey, 2003). If the external seawater has a lower Ω_{arag}, the coral may have to expend more energy for raising the internal Ω_{arag} to promote calcification in the extracellular calcifying medium (Cohen & Holcomb, 2009). Tropical corals obtain the energy required to move these ions mainly through symbiotic algal photosynthesis. It is possible that nubbins transplanted to the low Ω_{arag} ojo enhanced symbiont concentrations that provided more energy resources needed to

cope with the greater difference between the external and internal carbonate chemistry. Indeed, the higher symbiont concentrations may have allowed *S. siderea* nubbins transplanted to the ojo to maintain similar calcification rates than nubbins transplanted to the control site. Laboratory experiments with *Stylophora pistillata* have shown that calcification was maintained under high pCO_2 when symbiont content increased (Reynaud *et al.*, 2003), and it was reduced while symbiont concentration decreased (Krief *et al.*, 2010) or did not change (Tambutté *et al.*, 2015). It is also possible that photosynthates derived from endolithic algae may promote calcification under low Ω_{arag} because dense concentrations of endolithic algae have been related to higher survival of massive corals to bleaching events (Fine & Loya, 2002) and could also provide similar photosynthates to corals at low Ω_{arag}. Collectively, our data and data from these studies suggest that the energy provided by the symbionts can be used to overcome the larger gradient of proton and carbonate ion between the environment and the calcification solution in order to maintaining net growth at least in some coral species.

The chlorophyll *a* concentration per Symbiodiniaceae cell of *P. astreoides* and *S. siderea* was higher after 2 years of transplantation at low Ω_{arag} (Fig. 3.5), which suggests an increased capacity for photosynthetic activity that could provide additional energy to the corals. A higher concentration of chlorophyll *a* and net oxygen production was found in *Acropora formosa* under high CO_2 in a laboratory experiment (Crawley *et al.*, 2010). The increase in oxygen production may mean that more photosynthates are produced and assimilated by the host in such a manner the coral can keep

calcification rates under low Ω_{arag}. Nevertheless, further research is needed to elucidate the effects of low pH on chlorophyll *a* concentrations and assess the effect on calcification, since several authors have reported mixed results in laboratory experiments with *Stylophora pistillata* (Krief *et al.*, 2010; Reynaud *et al.*, 2003; Tambutté *et al.*, 2015). It is possible that the increase in chlorophyll *a* concentration is due to an increase in cyanobacteria that form the coral holobiont rather than Symbiodiniaceae; the cyanobacteria may promote photosynthesis through nitrogen fixation (Lesser *et al.*, 2004) and ultimately, provide the needed energetic resources to facilitate calcification under low Ω_{arag}.

The protein content per surface area was higher in *S. siderea* nubbins transplanted to the ojo vs. the control site (Fig. 3.5), suggesting that these corals may be thickening their organic matrix protein content to promote calcification under low Ω_{arag} seawater (Tambutté *et al.*, 2015). Several experimental studies have also reported an increase in host tissue and organic matrix protein concentrations under reduced pH in *Stylophora pistillata* and *Porites* sp. (Krief *et al.*, 2010; Tambutté *et al.*, 2015) and in *Oculina patagonica* and *Madracis pharensis* (Fine & Tchernov, 2007). While we did not measure tissue thickness, thicker tissue has been observed in low saturation corals at this field site (Crook *et al.*, 2013) and has been proposed to confer an advantage against coral bleaching (Hoegh-Guldberg, 1999; Loya *et al.*, 2001) and low pH (Rodolfo-Metalpa *et al.*, 2011), since it serves as a protective barrier against hot or corrosive seawater.

3.4.5 Shifting species assemblages in an acidified ocean

The differential sensitivity across populations and species to low Ω_{arag} suggest that, as ocean acidification progresses, the relative abundances of different coral species and populations in reef ecosystems may change towards dominance of slow-growing species, and hence changes in coral communities and reef structure are also likely, with potential cascading effects. This finding is particularly critical for reefs currently dominated by fast-growing, branching species, such as *Acropora* and *Stylophora pistillata* in Indo-Pacific shallow reefs (Hughes *et al.*, 2018). As sea level is expected to rise by 26 to 55 cm by 2100 (scenario RCP2.6, IPCC, Stocker, 2014), it is possible that coral reefs dominated by slow-growing species may not be able to grow fast enough to avoid drowning (Blanchon & Shaw, 1995). In addition, reduced skeletal density has been linked to increased bioerosion and boring (Crook *et al.*, 2013; DeCarlo *et al.*, 2015; Hoegh-Guldberg *et al.*, 2007) and low Ω_{arag} waters also weaken inorganic cementation of reef structures, which further promotes coral erosion (Manzello *et al.*, 2008) and leads to less cohesive reef frameworks that are more susceptible to storms.

In summary, while corals can calcify under ocean acidification conditions, the possible synergistic effects of sea level rise on slow growing corals; high temperature on Symbiodiniaceae concentrations; high nutrient concentrations on skeletal bioerosion; or increased storm intensity on less dense coral skeletons predict a challenging future for coral survival and growth. On the other hand, the differences in survival and calcification among coral species may be useful for studies of human-assisted evolution projects (van Oppen *et al.*, 2015) and implementation of restoration

programs as strategy to augment the capacity of reef organisms to tolerate stress and to facilitate recovery after disturbances.

3. 5 Figures

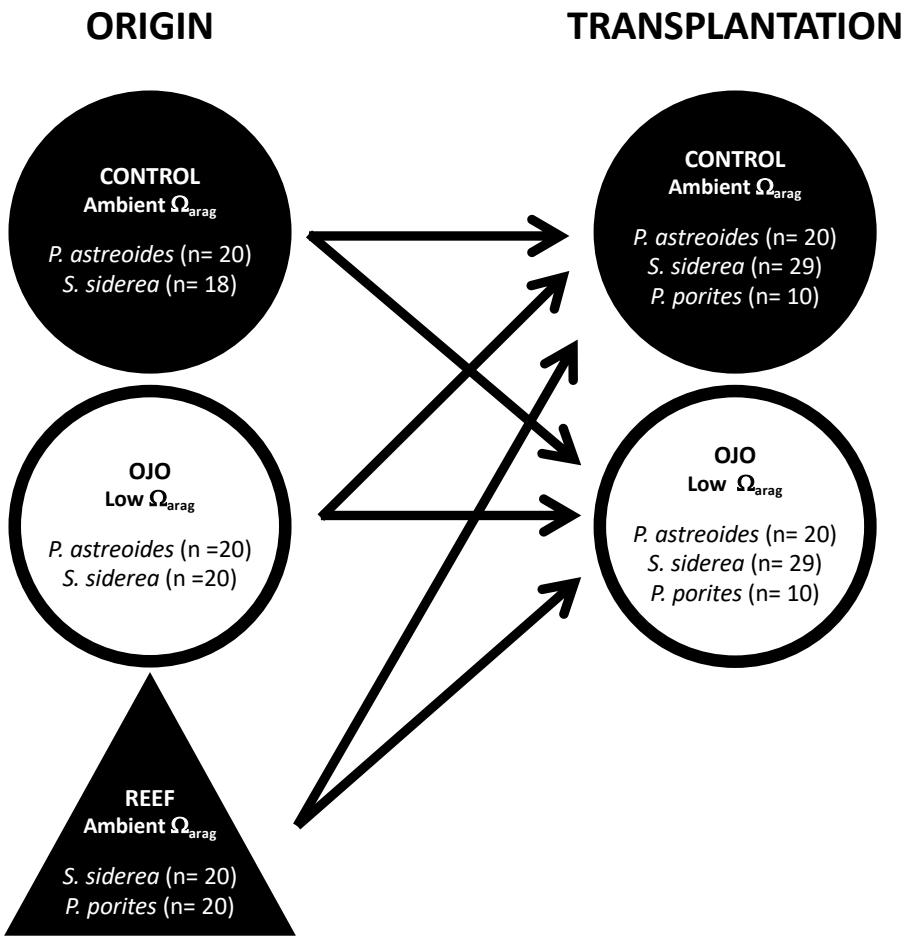

Figure 3.1. Transplant experiment design.

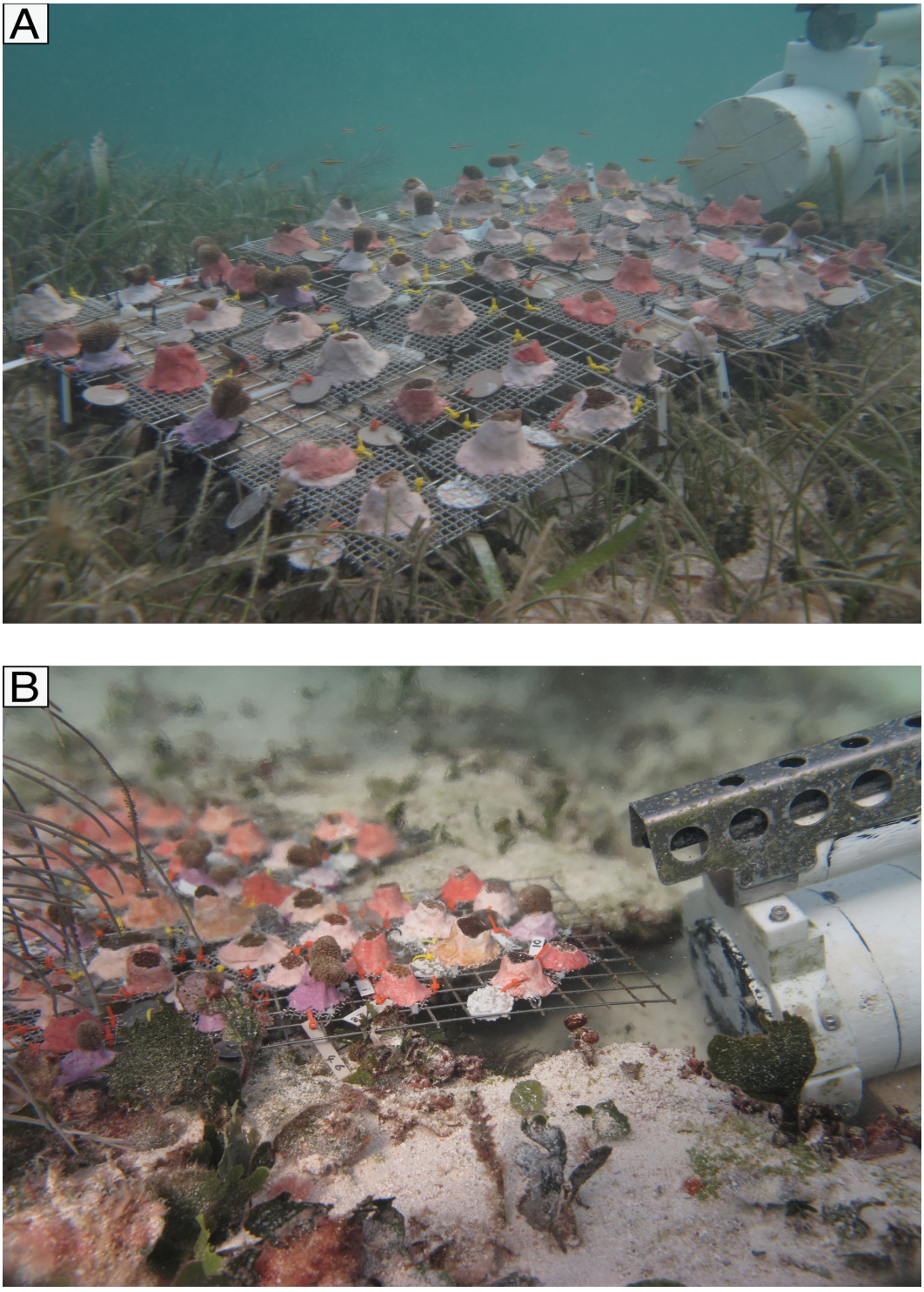

Figure 3.2. Transplanted nubbins at ambient Ω_{arag} control site (A) and at low Ω_{arag} ojo site (B). Credit: Yuichiro Takeshita.

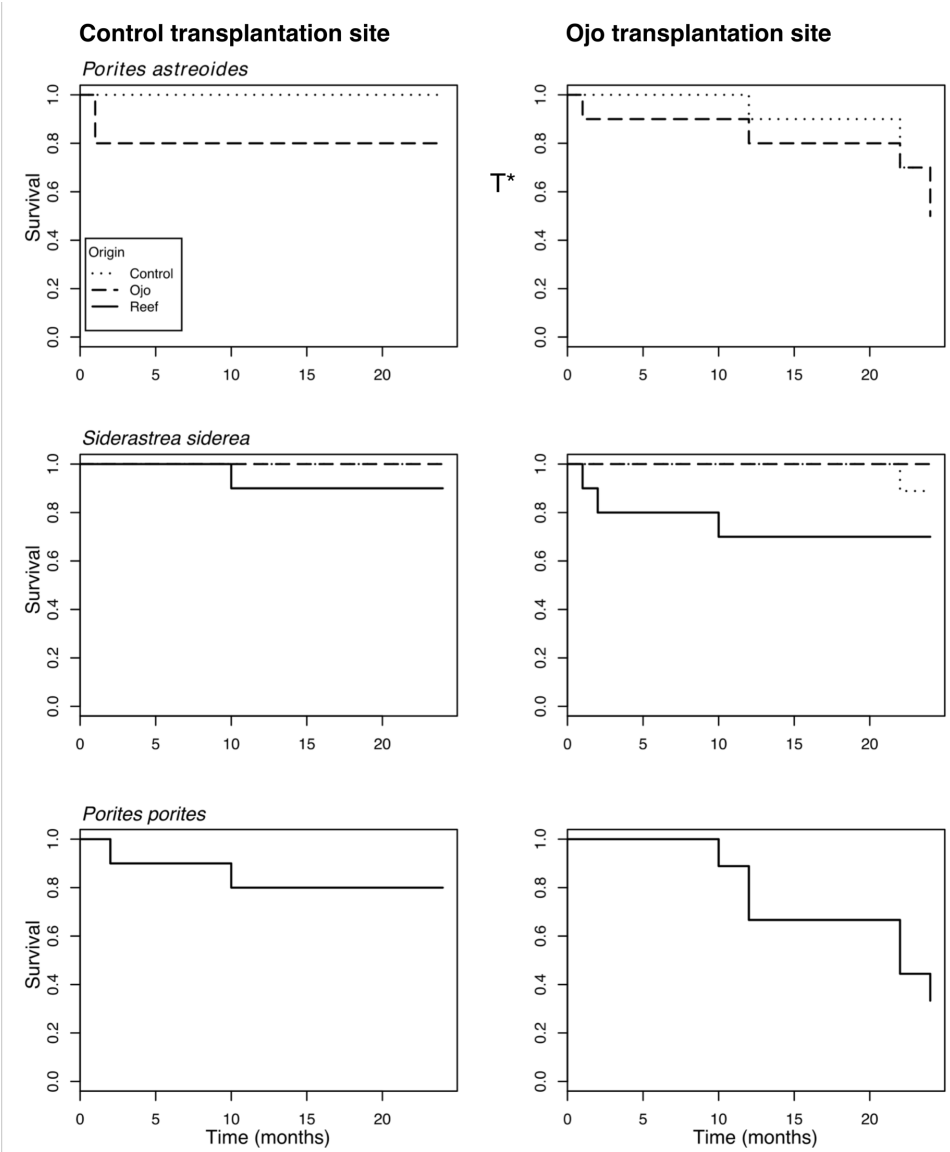

Figure 3.3. Survival curves of nubbins over 24 months after transplanting into ambient Ω_{arag} control site (left) and low Ω_{arag} ojo (right): *Porites astreoides* (n = 40), *Siderastrea siderea* (n = 58) and *Porites porites* (n = 19). Solid and dashed lines indicate collection origins of the corals. Asterisks indicate statistical significance at $p < 0.05$ (*), $p < 0.01$ (**) and $p < 0.001$ (***). Letters indicate overall comparisons of origin (O) and transplantation (T).

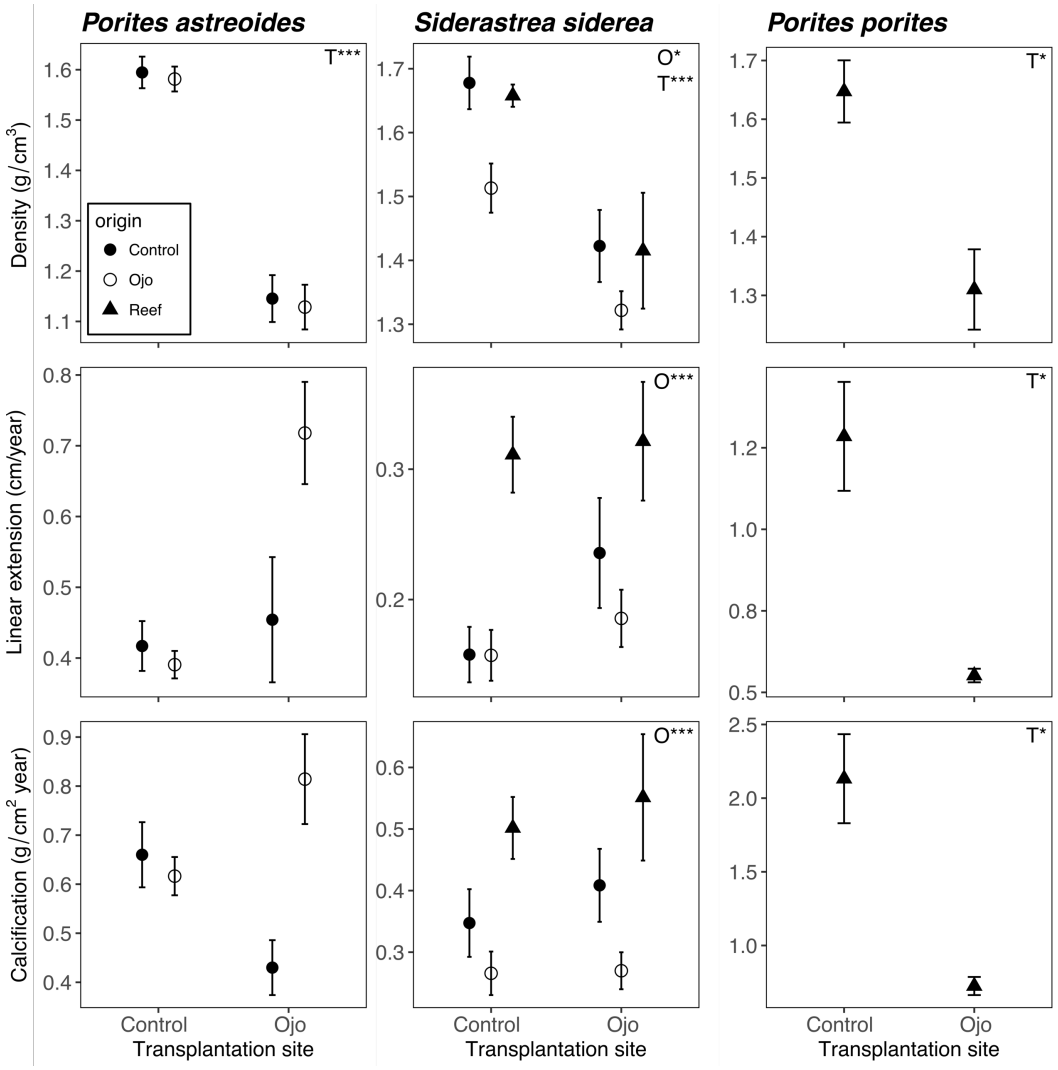

Figure 3.4. Bulk density, linear extension and calcification rates of skeletons deposited during the two years after transplantation. Symbols indicate collection origins. Note the different ranges on Y axes. Data are median ± SE. Letters and significance values are denoted as in Figure 3.3.

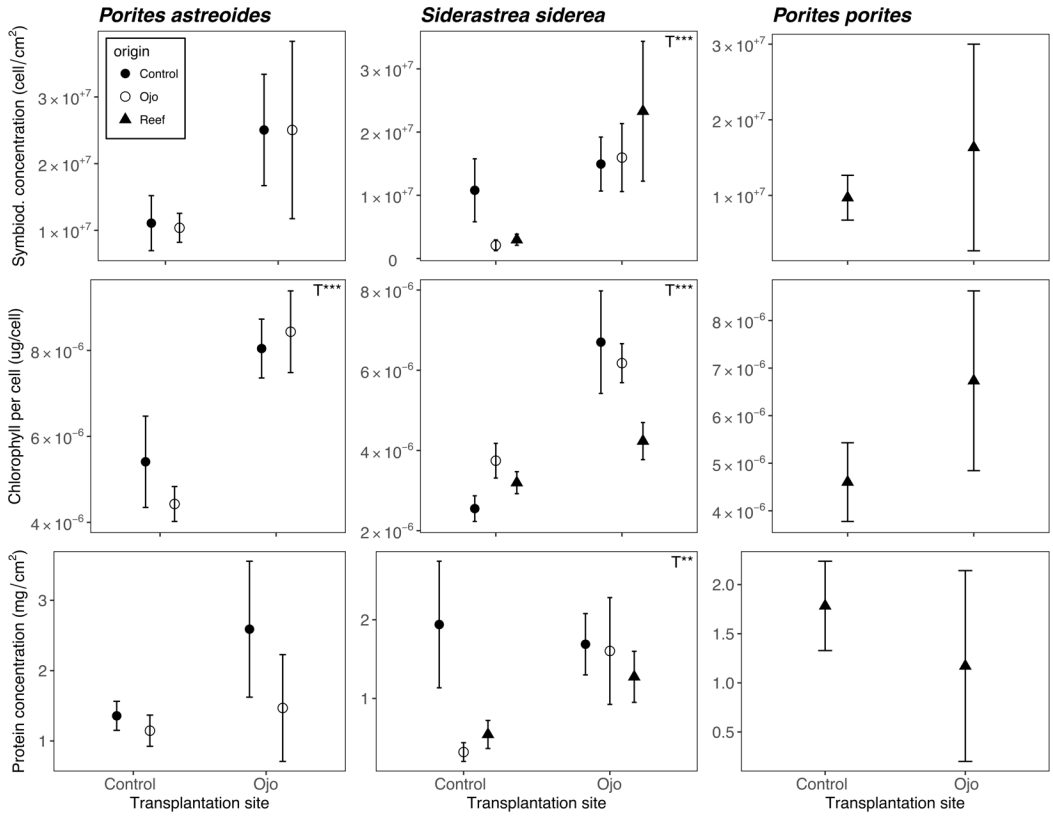

Figure 3.5. Symbiont, chlorophyll *a* and protein concentrations of surviving coral nubbins two years after transplantation at ambient Ω_{arag} control and low Ω_{arag} ojo sites. Data are median ± SE. Letters and significance values are denoted as in Figure 3.3.

3.6 Tables

Table 3.1. Numbers of colonies sampled from three coral species and three origins.

Number of colonies sampled				
Origin	*P. astreoides*	*S. siderea*	*P. porites*	Total
Control	10	9	0	19
Ojo	10	10	0	20
Reef	0	10	10	20
Total	20	29	10	59

Table 3.2. Numbers of nubbins from three coral species transplanted into two sites.

Number of nubbins transplanted				
Transplant site	*P. astreoides*	*S. siderea*	*P. porites*	Total
Control	20	29	10	59
Ojo	20	29	10	59
Total	40	58	20	118

Table 3.3 Chemistry parameters of water samples collected throughout the two-year experiment at control and ojo transplantation sites. Data are mean ± SE.
* Calculated using CO_2Sys.

Transplant site	N	Alkalinity (µmol kg^{-1})	DIC (µmol kg^{-1})	pH*	Ω_{arag}*	Temperature (°C)	Salinity
Control	15	2365 ± 32	2019 ± 12	8.17 ± 0.07	3.53 ± 0.43	26.9 ± 0.3	35.6 ± 0.1
Ojo	17	2759 ± 104	2621 ± 93	7.70 ± 0.14	2.10 ± 0.35	27.1 ± 0.2	33.2 ± 0.5

Chapter 4. Changes in gene expression in *Porites astreoides* after one year of transplantation to low aragonite saturation water

Abstract

Rising concentrations of atmospheric carbon dioxide and its dissolution in seawater decreases ocean pH and aragonite saturation state (Ω_{arag}), reducing the precipitation rate of calcium carbonate skeletons by corals. Coral responses to low pH, low Ω_{arag} conditions vary across species and populations, indicating differential resilience to ocean acidification. The molecular mechanisms that may allow corals to acclimate or adapt to ocean acidification are largely unknown. *Porites astreoides* is naturally found at low Ω_{arag} submarine springs along the Mexican Caribbean coast, suggesting a potential ability to acclimate to changing ocean carbonate chemistry. We collected nubbins of *P. astreoides* from low Ω_{arag} submarine springs and from ambient Ω_{arag} sites and reciprocally transplanted them to a low Ω_{arag} spring and an ambient Ω_{arag} control site. One year after transplantation, nubbins transplanted to the spring regulated genes involved in lipid metabolism, suggesting increased lipid breakdown for energy production to maintain calcification under low Ω_{arag}. Nubbins transplanted to the spring downregulated genes involved in bicarbonate transport, possibly impacting pH regulation and inorganic carbon supply at the calcification site. A candidate gene (Lrp6) putatively involved in coral calcification, and previously associated to low bone density in some animals, was also downregulated at the low Ω_{arag} spring. These gene expression

changes are consistent with the reported higher chlorophyll concentrations and reduced skeletal density seen in prior phenotypical analysis of *P. astreoides* nubbins after two years of transplantation to the low Ω_{arag} spring. These observations indicate that the regulation of lipid metabolism, bicarbonate transportation and expression of Lrp6 is linked to corals' capacity to calcify under ocean acidification conditions.

4.1 Introduction

Ocean carbonate chemistry is being altered by increasing concentrations of atmospheric carbon dioxide. Carbon dioxide dissolves in seawater decreasing the pH and carbonate saturation state of the ocean, resulting in ocean acidification (Caldeira & Wickett, 2003). The lower carbonate saturation state impacts marine organism that precipitate calcium carbonate skeletons (Raven *et al.*, 2005). Calcification of scleractinian corals is expected to decline as dissolved CO_2 increases and Ω_{arag} of seawater decreases (Gattuso *et al.*, 1998; Kleypas *et al.*, 1999). Many laboratory experiments have reported reduced coral growth under ocean acidification conditions (e.g.: Chan & Connolly, 2013; Cohen *et al.*, 2009; Krief *et al.*, 2010); however, corals have been found living at low pH vents (Fabricius *et al.*, 2011) and submarine springs (Crook *et al.*, 2012). Therefore, some coral species can survive and calcify under low Ω_{arag} although the molecular mechanisms behind this remain poorly understood.

Coral calcification involves the transportation of calcium and inorganic carbon across membranes and requires supersaturation at the calcification site to precipitate calcium carbonate (Allemand *et al.*, 2011; Cohen & Holcomb, 2009). The majority of

inorganic carbon used in coral calcification comes from metabolic CO_2 (Furla *et al.*, 2000), which is converted into bicarbonate ions through a reversible reaction catalyzed by the enzyme carbonic anhydrase (CA). While CO_2 diffuses through membranes, active transport of membrane-impermeable bicarbonate ions via transmembrane proteins is needed to promote calcification (Zoccola *et al.*, 2015). The calcification process produces protons that are removed from the calcifying medium to maintain supersaturated conditions (Cohen & Holcomb, 2009; Jokiel, 2011). The plasma membrane Ca_2^+-ATPase removes protons from the calcifying medium while using ATP (Al-Horani *et al.*, 2003; Cohen & McConnaughey, 2003; McConnaughey & Whelan, 1997). Other potential proton transporters, such as vacuolar-type proton ATPase, may also be involved in proton pumping, although their role remains unknown (Allemand *et al.*, 2004; Tresguerres, 2016). Some laboratory studies with corals maintained under high pCO_2 have reported upregulation of proton transporters in *Siderastrea siderea* (Davies *et al.*, 2016); and of calcium and bicarbonate transporters and CA in *Pocillopora damicornis* (Vidal-Dupiol *et al.*, 2013). In contrast, other studies have reported downregulation of CA in experiments with *Acropora millepora* (Moya *et al.*, 2012; Ogawa *et al.*, 2013) and *A. aspera* (Moya *et al.*, 2012; Ogawa *et al.*, 2013) and of V-type proton ATPase in *A. millepora* (Kaniewska *et al.*, 2012). The downregulation of calcification-related genes in *A. millepora* seem to disappear when exposure time to high pCO_2 is extended (Kenkel *et al.*, 2018; Moya *et al.*, 2015; Rocker *et al.*, 2015). However, it is not clear if corals can acclimate to *in-situ* ocean acidification conditions after transplantation and if some molecular responses can promote calcification under low Ω_{arag}.

To investigate the acclimation potential of *Porites astreoides* to ocean acidification *in-situ* and the concomitant shifts in gene expression, we transplanted 20 nubbins to a low Ω_{arag} submarine spring and 20 at an ambient Ω_{arag} control site (Chapter 3). Low pH saline groundwater discharges along the Caribbean coast of the Yucatan Peninsula (Mexico), forming submarine springs (locally called "ojos") that serve as a natural laboratory to study the impacts of low Ω_{arag} seawater on coral calcification. *P. astreoides* is naturally found at the ojos (Crook *et al.*, 2012) although the skeletal density and calcification rates of these corals are lower than colonies of the same species living at ambient Ω_{arag} (Crook *et al.*, 2013). After 1 year of transplantation, tissue samples were collected for transcriptomic analyses and after 2 years of transplantation, surviving nubbins were collected for physiological analyses (Chapter 3). Sixty percent of nubbins survived at the ojo while 90% survived at the control transplantation site. Nubbins transplanted to the ojo had lower skeletal density but maintained net linear extension and calcification rate (Chapter 3). Nubbins transplanted to the ojo also had higher chlorophyll concentrations, suggesting increased symbiont photosynthetic activity under low Ω_{arag} (Chapter 3). In this study, we compare gene expression of the nubbins transplanted to the low Ω_{arag} ojo to those transplanted to ambient Ω_{arag} control sites after one year of transplantation.

4.2 Materials and methods

4.2.1 Study area

Saline groundwater discharges along the Caribbean coast of the Yucatan peninsula, Mexico, at submarine springs ("ojos"). The water discharging at the ojos is

characterized by lower than ambient pH and Ω_{arag} and higher than ambient total inorganic carbon and total alkalinity. The salinity and temperature are generally close to ambient values although they fluctuate diurnally and seasonally (Hofmann *et al.*, 2011). The average values for physicochemical parameters of water sampled at the ojo and control transplantation sites during the experiment can be found in Table 3.3 from Chapter 3. Additional data including salinity, temperature and pH obtained from sensors deployed at the site has been previously published (Crook *et al.*, 2012; Crook *et al.*, 2013; Crook *et al.*, 2016; Hofmann *et al.*, 2011; Null *et al.*, 2014; Paytan *et al.*, 2014).

4.2.2 Coral sampling and transplant experiment

Twenty colonies of *P. astreoides* were sampled with a pneumatic drill corer attached to a scuba tank. Ten colonies were collected at ojos and 10 colonies were obtained from nearby (~ 2 m away) control sites not directly affected by ojo discharge. Two genetically identical nubbins (~3 cm diameter; ~2-3 cm long) were extracted from each colony (total N = 40). One nubbin from each colony was transplanted to the low Ω_{arag} ojo and the second nubbin was transplanted to ambient Ω_{arag} control site (~ 5 m away from the ojo). After one year of transplantation, 11 of the nubbins (5 from ojo and 6 from control transplantation sites) were sampled by divers for gene expression analysis (see Table 4.1 for collection and transplantation details). A piece of each nubbin (~ 1 cm^3) was removed, placed in a 20 ml plastic vial with RNAlater and preserved at -80 °C until further analysis.

4.2.3 mRNA extraction and sequencing

Each nubbin piece was crushed with liquid nitrogen in a mortar and RNA was extracted with TRIzol (Invitrogen/ Life Technologies) using a modified protocol described in Barshis *et al.* (2013). RNA yield was quantified with a Qubit 2.0 fluorometer (Invitrogen/ Life Technologies). Libraries were prepared with the Illumina TruSeq™ RNA Sample Prep Kit v2 following manufacturer's protocols in the Barshis lab at Old Dominion University. Unique adapters were ligated to identify each sample. The quantity and quality of cDNA libraries were determined with a Qubit 2.0 fluorometer and a Fragment Analyzer automated CE system (Advanced Analytical Technologies), respectively. One lane with the 11 samples of *P. astreoides* was run with a 150 bp single-end read sequencing in an Ilumina HiSeq2500 Rapid platform at Vincent J. Coates Genomics Sequencing Laboratory (University of California, Berkeley).

4.2.4 *De novo* assembly of coral transcriptome

Sequenced data was processed following the steps described in Barshis *et al.*, (2013) and De Wit *et al.* (2012). A custom script was used to trim reads shorter than 20 bases, and raw sequences with bases with a Phred quality score lower than 20 over 90% of the sequence. Cutadapt (Martin, 2011) was used to clip Illumina adapter sequences and trim subsequent low-quality bases from the end of the reads. The quality trimmed sequences were *de novo* assembled using Trinity software and default parameters (version 2.0.6; Grabherr *et al.*, 2011) to create a reference transcriptome.

4.2.5 Annotation

The *de novo* assembled contigs were BLASTN against four nucleotide databases as described in Barshis *et al.* (2013) and Ladner & Palumbi (2012) to identify putative cnidarian and symbiont sequences.

The 18,001 contigs from *P. astreoides* assembly that putatively matched to cnidarian-specific nucleotide sequences were aligned with BLASTX against three protein databases: the NCBI nonredundant protein database (nr; www.ncbi.nlm.nih.gov) and against the Uniprot Swiss-Prot and TrEMBL protein databases (www.uniprot.org) with an *e* value cutoff of $\leq 1 \times 10^{-4}$. The sequences were annotated and then associated to gene ontology (GO) categories and protein function descriptions as described in De Wit *et al.* (2012) and Barshis *et al.* (2013)

4.2.6 Mapping

An assembly was created by combining the putative cnidarian and *Symbiodinium de novo* assemblies to use as a mapping reference. High quality forward reads from each sample were mapped against the combined assemblies using Burrow's-Wheeler aligner and default parameters (version 0.7.12-r1039).

4.2.7 Gene expression and functional enrichment analyses

The aligned reads that mapped uniquely to each contig of the reference assembly for ≥20 bp with a mapping quality of ≥20 were counted. The counted mapping data was analyzed with the DESeq2 package in R (Anders & Huber, 2010) to

measure differential gene expression based on the negative binomial distribution. The read counts were normalized and only contigs with a mean normalized expression > 5 and a False Discovery Rate adjusted *p*-value < 0.1 (Benjamini & Hochberg, 1995) were identified as significantly differentially expressed genes. Heatmaps of differentially expressed contigs ($p < 0.05$) were produced to visualize differences among samples. Functional enrichment analysis was performed with ErmineJ (version 3.0.2) to determine overrepresented gene ontology categories based on Benjamini-Hochberg assessment p-values (FDR < 0.1).

4.3 Results

4.3.1 Transcriptome assembly

The transcriptome assembly of *P. astreoides* had 80,565 contigs comprising 27,989,282 bases. 22.3% of these contigs were identified as putatively cnidarian (18,001 contigs). 8,975 of the annotated 18,001 cnidarian contigs had no description. The final reference transcriptome had 19,195 contigs with an average length of 393 bases, N50 of 398 bases and a total number of 7,549,972 bases.

4.3.2 Differentially expressed genes

Out of the 7,243 contigs with base mean >5, 261 genes were differentially expressed between nubbins transplanted to the ojo (n = 5) and control (n = 6) sites (Fig. 4.1). Ninety-seven genes were upregulated (1.3%, $\log_2$ fold change range: 0.67 to 4.07) and 164 genes were downregulated (2.3%, $\log_2$ fold change range: -0.80 to -7.49) in the ojo transplants compared to the control transplants. The highest upregulated gene

(TR14958, *q* - value: 1.26 x10^{-8}, fold change: 4.07) annotated to an uncharacterized protein (ECO:0000313|EMBL: EOA12222.1). The most differentially downregulated contig (TR53224, q-value= 1.28 x10^{-4}, fold change: -3.07) was also annotated to an uncharacterized protein (ECO:0000313|EMBL: ERG85751.1) in the GO:0016021. This gene ontology corresponds to an integral component of the membrane.

4.3.3 Functional enrichment analysis

There were 23 gene sets that were overrepresented after functional enrichment analysis (FDR<0.1, Table 4.2). The most overrepresented gene sets are the cellular components "anchored component of membrane" set (GO:0031225) and "anchored component of plasma membrane" set (GO:0046658). Most of the differentially expressed contigs in these two gene sets encode MAM domain-containing glycosylphosphatidylinositol anchor protein 1. These contigs are downregulated in corals transplanted to the ojo (Fig. 4.2) and encode a protein involved in neuron migration and synapses (Lee *et al.*, 2013). These contigs are also present in the GO:0001764 (neuron migration).

The highest overrepresented biological process gene sets were four gene sets involved in the regulation of bile acid biosynthetic and metabolic processes (GO:0070857, GO:0070858, GO:1904251 and GO:1904252; Table 4.2) constituted by the same 14 contigs encoding MAM and LDL receptor class A domain containing protein 1 (Fig. 4.3). These contigs were present in the rest of the biological process gene sets involving lipid (cholesterol, sterol, steroid) homeostasis, biosynthesis and

metabolism and ketone metabolic process. Genes that encode ATP-binding cassette sub-family A member 1 and 2 in the GO:0055088 (lipid homeostasis), GO:0055092 (sterol homeostasis) and GO:0042632 (cholesterol homeostasis) were downregulated at the low Ω ojo (Fig. 4.3).

The molecular function gene sets that are overrepresented are cargo and steroid hormone receptor activity (GO:0038024 and GO:0003707; Table 4.2) and lipid transporter activity (GO:0005319). Two contigs of the steroid hormone receptor activity gene set have been identified as nuclear receptors in *Acropora millepora* (AmNR8 and AmNR4 isoform B) and are downregulated in corals transplanted to the ojo.

4.3.4 Calcification-related genes

There was no overrepresentation of the gene sets related to carbonic anhydrase (GO:0004089 - carbonate dehydratase activity), plasma membrane calcium ATPase (GO:0005388 – calcium-transporting ATPase activity), or proton pumping vacuolar ATPase (GO:0033176 – proton -transporting V-type ATPase complex) (Fig. 4.4) in corals transplanted to the ojo. Several genes included in the bicarbonate transmembrane transporter activity gene set (GO:0015106) and the regulation of bone remodeling gene set (GO:0046850) were downregulated in nubbins transplanted to the ojo (Fig. 4.4).

4.4 Discussion

4.4.1 Nubbins transplanted to low Ω_{arag} regulated genes involved in lipid metabolism

The overrepresentation of gene sets and differential expression of genes related to bile acid and cholesterol regulation in *P. astreoides* nubbins transplanted to the ojo indicates enhanced lipid metabolism under low Ω_{arag} conditions. Corals transplanted to the ojo downregulated genes encoding MAM and LDL-receptor class A domain-containing protein 1 (MALRD1) (Fig. 4.3). This protein increases the synthesis of fibroblast growth factor in humans (FGF19) and mice (FGF15), which inhibits the production of bile acid (Shapiro *et al.*, 2018; Vergnes *et al.*, 2013). Bile acid solubilizes stored lipids (triglycerides) to promote their conversion into fatty acids by lipases. These fatty acids are catabolized through beta-oxidation into acetyl-CoA to be used in the Citric acid cycle in the mitochondria to produce energy (Houten & Wanders, 2010). Therefore, the downregulation of MALRD1 suggests an increase in bile acid synthesis, which digests stored fat into an absorbable form of energy.

In addition, ATP binding cassette subfamily A member 1 (ABCA1), which encodes a transmembrane protein responsible for removing cholesterol out of the cell cytoplasm (Schmitz & Langmann, 2001), was also downregulated in nubbins transplanted to the ojo (Fig. 4.3). It has been shown that downregulation of ABCA1 led to an accumulation of cholesterol in the cytoplasm in other scenarios (Sene *et al.*, 2013). Cholesterol accumulation promotes bile acid synthesis, and the first step of this reaction is catalyzed by the enzyme cholesterol 7alpha-hydroxylase encoded by the regulatory

gene CYP7A1 (Russell, 2003). CYP7A1 is inhibited by FGF19 (Chiang, 2009) and upregulated by an increase in cholesterol concentration, therefore inducing the conversion of cholesterol into bile acid when more cholesterol is available.

The downregulation of both MALDR1 and ABCA1 suggests that bile acid synthesis is increasing after transplantation to ojo, facilitating the digestion of lipids. Lipids among other functions are used as an important energy reserve, containing over twice as much energy per gram as carbohydrates (caloric values: lipids: -39.5 kJ g^{-1}, proteins: −23.9 kJ g^{-1}, and carbohydrates: −17.5 kJ g^{-1}; Gnaiger & Bitterlich, 1984), hence the differential expression of genes related to lipid storage and metabolism may indicate that the corals acclimation response is related to energy acquisition. Calcification is an energetically costly mechanism that can take up to 30% of the coral's energy budget (Allemand *et al.*, 2011). A decline in external Ω_{arag} seawater requires corals to increase proton pumping out of the calcifying fluid to keep aragonite supersaturation at the calcification site, with a consequent increase in energy demand (Cohen & Holcomb, 2009). Therefore, corals growing under low Ω_{arag} conditions may increase lipid breakdown to use it as an energy source.

Our results are consistent with some observations from corals maintained under high pCO_2 in controlled laboratory experiments. Glycogen synthase and glycogen phosphorylase genes were downregulated in *Acropora aspera*, suggesting a reduction in glucose storage after two weeks and use of stored lipids as a source of energy (Ogawa *et al.*, 2013). In addition, lipolysis and beta-oxidation metabolic pathways were

upregulated in *Acropora millepora* (Kaniewska *et al.*, 2012) and *Pocillopora damicornis* (Vidal-Dupiol *et al.*, 2013), indicating increased breakdown of lipid reserves for energy production under elevated pCO_2. In contrast, differential expression of genes leading to lipid storage was observed in *Acropora millepora* collected from high pCO_2 seeps (Kenkel *et al.*, 2018). Increase in lipid concentration has also been reported in *Acropora cervicornis* (Towle *et al.*, 2015), *Acropora millepora* and *Pocillopora damicornis,* but not in *Montipora monasteriata* and *Turbinaria reniformis* (Schoepf *et al.*, 2013) maintained under high pCO_2 in laboratory experiments. These conflicting results among studies may be due to variable experimental methods or biological mechanisms. Differential metabolic activity, feeding rate, photosynthesis rate and/or photosynthate assimilation under low pH may all impact lipid storage and usage. In fact, the chlorophyll concentration of *P. astreoides* nubbins transplanted to the ojo was higher than that of nubbins transplanted to the control site, suggesting an elevated symbiont photosynthetic activity, and possibly more energy translocated to the host. The variability in lipid metabolism and energy allocation may be responsible for the differential coral resilience and growth seen under diverse ocean acidification experimental and environmental settings.

4.4.2 Nubbins transplanted to low Ω_{arag} downregulated genes associated to bicarbonate transport and skeletal density

Calcification-related gene sets were not enriched, and genes associated with carbonic anhydrases, Ca -ATPase and V-type ATPase were not differentially expressed among transplantation sites (Fig. 4.4). In addition to proton pumping, pH and Ω_{arag}

elevation at the calcifying medium could be achieved by bicarbonate transportation to the site of calcification (Zoccola *et al.*, 2015). Interestingly, the solute carrier family 26 member 6 (SLC26), which is responsible for bicarbonate transmembrane transportation, was downregulated in corals transplanted to low Ω_{arag} (Fig. 4.4). Bicarbonate is a membrane-impermeable ion that can be converted into CO_2 by carbonic anhydrase to be used in photosynthesis or it can be converted into carbonate ions to be used in calcification. SLC26 bicarbonate transporter has been found ubiquitously expressed in both the oral tissue where symbionts are located and in the aboral tissue, next to the calcification site (Zoccola *et al.*, 2015). SLC26 can bind to cytosolic CA to form a transport metabolon which maximizes bicarbonate transport rate (Alvarez *et al.*, 2005). Therefore, while there was no downregulation of CA in corals transplanted to low Ω_{arag}, a downregulation of SLC26 may indicate a reduction in the inorganic carbon supply for calcification or photosynthesis. In fact, SLC26 was down-regulated 92-fold in bleached *P. astreoides* after 6 weeks of thermal stress (Kenkel *et al.*, 2013). While it is not possible to distinguish if a downregulation of bicarbonate transporters impacts photosynthesis or calcification or both, a reduction in photosynthesis will ultimately affect coral calcification. The downregulation of chloride anion exchanger (SLC26A3) and anion exchange protein 4 (SLC4A9) (Fig. 4.4), which are also bicarbonate/chloride transporters (Cordat & Casey, 2009) further supports the hypothesis of a link between bicarbonate transport and reduced calcification in the low Ω_{arag} transplants.

The downregulation of low-density lipoprotein receptor-related protein 6 (Lrp6) in nubbins transplanted to the ojo (Fig. 4.4) may indicate an impact on skeletal development. Lrp6 regulates bone formation and resorption (Kang & Robling, 2015) and mutations in this gene have been associated with low bone mineral density in mice (Holmen *et al.*, 2004; Kokubu *et al.*, 2004) and osteoporosis in humans (Mani *et al.*, 2007). Therefore, the downregulation of Lrp6 may play role in the reduced skeletal density seen at the phenotypic level of nubbins transplanted to low Ω_{arag} ojo (Chapter 3). Reduced skeletal density and increased porosity have also been reported in *P. astreoides* cores collected from ojos (Crook *et al.*, 2013), in *Porites* cores collected from Pacific reefs (Mollica *et al.*, 2018), in temperate *Balanophyllia europaea* collected from Mediterranean CO_2 vents (Fantazzini *et al.*, 2015), and in *Stylophora pistillata* grown under high pCO_2 in a year-long laboratory experiment (Tambutté *et al.*, 2015). Further exploration of the role of Lrp6 on coral calcification is required to elucidate the molecular mechanisms underlying the "coral osteoporosis" found in several coral species across diverse settings.

This study reports a shift in expression of genes involved in lipid metabolism and calcification of *P. astreoides* nubbins after one year of in-situ transplantation to a low Ω_{arag} ojo. Metabolic genes conducive to the breakdown of lipid reserves for energy production were differentially expressed at low Ω_{arag}, suggesting an elevated energy demand to sustain calcification under ocean acidification conditions. Genes involved in bicarbonate transport were downregulated at low Ω_{arag}, signifying the putative role of bicarbonate in elevating the inorganic carbon supply and pH at the calcification site

to promote calcium carbonate production. A candidate gene potentially responsible for low skeletal density was also downregulated, in agreement with the reduced skeletal density found in nubbins transplanted to the ojo. The ability of corals to regulate these genes may determine their resilience to future changes in ocean carbonate chemistry.

4.5 Figures

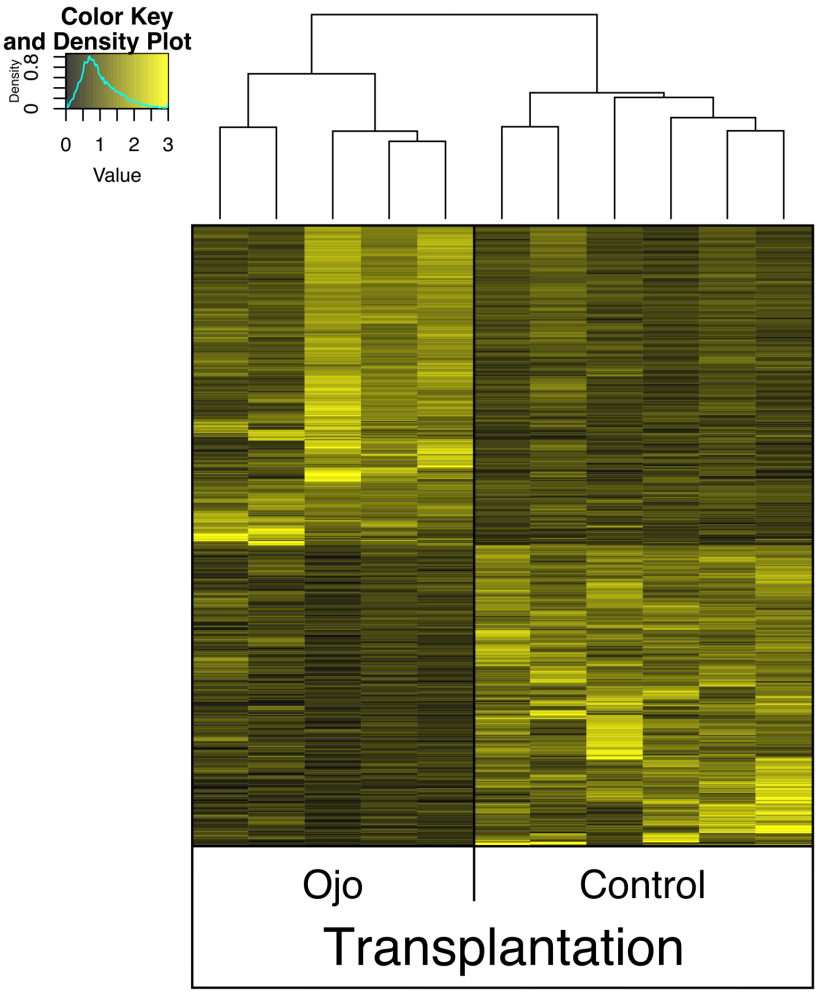

Figure 4.1. Heatmap of differential gene expression of nubbins transplanted to low Ω_{arag} ojo (n = 5) and ambient Ω_{arag} control site (n = 6).

Transplantation Ojo	Transplantation Control	Contig	p value	Name	Gene Ontology
		TR49214	0.000231	MAM domain-containing glycosylphosphatidylinositol anchor protein 1	GO:0031225. Anchored component of membrane
		TR1516	0.000778	MAM domain-containing glycosylphosphatidylinositol anchor protein 1	
		TR35173	0.00116	MAM domain-containing glycosylphosphatidylinositol anchor protein 1	
		TR37980	0.00131	MAM domain-containing glycosylphosphatidylinositol anchor protein 1	
		TR48329	0.00259	MAM domain-containing glycosylphosphatidylinositol anchor protein 1	
		TR5119	0.00277	Neuronal growth regulator 1	
		TR46453	0.00491	MAM domain-containing glycosylphosphatidylinositol anchor protein 1	
		TR21541	0.00503	MAM domain-containing glycosylphosphatidylinositol anchor protein 1	
		TR13105	0.00720	MAM domain-containing glycosylphosphatidylinositol anchor protein 1	
		TR37854	0.00950	MAM domain-containing glycosylphosphatidylinositol anchor protein 1	
		TR47126	0.0199	MAM domain-containing glycosylphosphatidylinositol anchor protein 1	
		TR13756	0.0254	MAM domain-containing glycosylphosphatidylinositol anchor protein 1	
		TR1919	0.0257	MAM domain-containing glycosylphosphatidylinositol anchor protein 1	
		TR58422	0.0385	Uromodulin	
		TR65181	0.0392	Contactin-5	
		TR8925	0.0548	MAM domain-containing glycosylphosphatidylinositol anchor protein 1	
		TR64841	0.0988	Melanotransferrin	

Figure 4.2. Enriched gene set containing cellular component genes.

Transplantation Ojo	Transplantation Control	Contig	p value	Name	Gene Ontology
		TR58347	6.80e-05	MAM and LDL-receptor class A domain-containing protein 1	GO:0070857. Regulation of bile acid biosynthetic process
		TR65879	0.000128	MAM and LDL-receptor class A domain-containing protein 1	
		TR53761	0.00140	MAM and LDL-receptor class A domain-containing protein 1	
		TR69596	0.00210	MAM and LDL-receptor class A domain-containing protein 1	
		TR33379	0.00519	MAM and LDL-receptor class A domain-containing protein 1	
		TR66372	0.00539	MAM and LDL-receptor class A domain-containing protein 1	
		TR56377	0.00878	MAM and LDL-receptor class A domain-containing protein 1	
		TR58	0.0156	MAM and LDL-receptor class A domain-containing protein 1	
		TR53704	0.0316	MAM and LDL-receptor class A domain-containing protein 1	
		TR54344	0.0442	MAM and LDL-receptor class A domain-containing protein 1	
		TR49785	0.0743	MAM and LDL-receptor class A domain-containing protein 1	
		TR38708	0.0874	MAM and LDL-receptor class A domain-containing protein 1	
		TR58347	6.80e-05	MAM and LDL-receptor class A domain-containing protein 1	GO:0042632. Cholesterol homeostasis
		TR65879	0.000128	MAM and LDL-receptor class A domain-containing protein 1	
		TR53761	0.00140	MAM and LDL-receptor class A domain-containing protein 1	
		TR69596	0.00210	MAM and LDL-receptor class A domain-containing protein 1	
		TR33379	0.00519	MAM and LDL-receptor class A domain-containing protein 1	
		TR66372	0.00539	MAM and LDL-receptor class A domain-containing protein 1	
		TR60507	0.00567	ATP-binding cassette sub-family A member 1	
		TR56377	0.00878	MAM and LDL-receptor class A domain-containing protein 1	
		TR58	0.0156	MAM and LDL-receptor class A domain-containing protein 1	
		TR62172	0.0268	ATP-binding cassette sub-family A member 2	
		TR53704	0.0316	MAM and LDL-receptor class A domain-containing protein 1	
		TR54344	0.0442	MAM and LDL-receptor class A domain-containing protein 1	
		TR14880	0.0450	Low density lipoprotein receptor adapter protein 1	
		TR49785	0.0743	MAM and LDL-receptor class A domain-containing protein 1	
		TR38708	0.0874	MAM and LDL-receptor class A domain-containing protein 1	

Figure 4.3. Enriched GO categories containing genes involved in the regulation of bile acid biosynthetic process and cholesterol homeostasis.

Transplantation Ojo | Control	Contig	p value	Name	Gene Ontology
	TR12509	0.280	Carbonic anhydrase 12	GO:0004089. Carbonate dehydratase activity
	TR12535	0.558	Carbonic anhydrase	
	TR45572	0.105	Sarcoplasmic/endoplasmic reticulum calcium ATPase 2	GO:0005388. Calcium - transporting ATPase activity
	TR1598	0.139	Protein retinal degeneration B	
	TR72131	0.173	Plasma membrane calcium-transporting ATPase 2	
	TR2808	0.524	Plasma membrane calcium-transporting ATPase 2	
	TR2341	0.554	Plasma membrane calcium-transporting ATPase 3	
	TR28340	0.751	Plasma membrane calcium-transporting ATPase 3	
	TR12263	0.931	Plasma membrane calcium-transporting ATPase 4	
	TR29338	0.993	Calcium-transporting ATPase type 2C member 1	
	TR68456	1.00	Plasma membrane calcium-transporting ATPase 2	
	TR64867	1.00	Calcium-transporting ATPase sarcoplasmic/endoplasmic...	
	TR2153	1.00	Plasma membrane calcium-transporting ATPase 4	
	TR38386	0.245	V-type proton ATPase catalytic subunit A	GO:0033176. Proton - transporting V-type ATPase complex
	TR56263	0.297	Probable V-type proton ATPase subunit H 2	
	TR67770	0.432	V-type proton ATPase catalytic subunit A isoform 2	
	TR68955	0.506	V-type proton ATPase 116 kDa subunit a isoform 1	
	TR65759	0.554	V-type proton ATPase catalytic subunit A	
	TR63161	0.714	Predicted protein {ECO:0000313|EMBL:EDO39520.1}	
	TR28590	0.816	V-type proton ATPase subunit H	
	TR5404	0.969	Predicted protein {ECO:0000313|EMBL:EDO39520.1}	
	TR5361	1.00	V-type proton ATPase subunit C 1-B	
	TR24172	1.00	V-type proton ATPase 21 kDa proteolipid subunit	
	TR5160	0.00897	Solute carrier family 26 member 6	GO:0015106. Bicarbonate transmembrane transporter activity
	TR29725	0.0421	Chloride anion exchanger	
	TR24747	0.0546	Anion exchange protein 4	
	TR28302	0.122	Electroneutral sodium bicarbonate exchanger 1	
	TR7683	0.136	Sodium bicarbonate transporter-like protein 11	
	TR18156	0.185	Sodium bicarbonate cotransporter 3	
	TR5373	0.267	Electrogenic sodium bicarbonate cotransporter 1	
	TR39345	0.720	Sodium bicarbonate cotransporter 3	
	TR6127	1.00	Solute carrier family 26 member 6	
	TR309	0.000856	Low-density lipoprotein receptor-related protein 6	GO:0046850. Regulation of bone remodeling
	TR56534	0.0179	P2X purinoceptor 7	
	TR48072	0.0414	Low-density lipoprotein receptor-related protein 4	
	TR47761	0.125	Low-density lipoprotein receptor-related protein 5	
	TR55028	0.136	SUN domain-containing ossification factor	
	TR57849	0.487	Low-density lipoprotein receptor-related protein 6	
	TR6120	0.717	Integrin alpha-V	
	TR3339	0.726	"Type II inositol 3,4-bisphosphate 4-phosphatase"	
	TR58175	0.749	Neurofibromin	
	TR38513	0.908	Low-density lipoprotein receptor-related protein 6	

Figure 4.4. Gene ontologies containing calcification-related genes.

4.6 Tables

Table 4.1. Origin and transplantation details of *P. astreoides* nubbins sampled and sequenced after 1 year of reciprocal transplant experiment.

Origin	**Transplant site**	**N**
Control	Control	3
	Ojo	2
Ojo	Control	3
	Ojo	3

Table 4.2. Enriched gene ontology categories of *Porites astreoides*.

ID	Name	# genes	p value	Q value	Same as
GO:0031225	anchored component of membrane	44	1.00E-12	2.78E-09	
GO:0046658	anchored component of plasma membrane	19	1.00E-12	1.39E-09	
GO:0070857	regulation of bile acid biosynthetic process	14	1.00E-12	9.28E-10	GO:1904252, GO:1904251, GO:0070858
GO:0070858	negative regulation of bile acid biosynthetic process	14	1.00E-12	9.28E-10	GO:1904252, GO:1904251, GO:0070857
GO:1904251	regulation of bile acid metabolic process	14	1.00E-12	9.28E-10	GO:1904252, GO:0070857, GO:0070858
GO:1904252	negative regulation of bile acid metabolic process	14	1.00E-12	9.28E-10	GO:1904251, GO:0070857, GO:0070858
GO:0042632	cholesterol homeostasis	43	5.00E-06	3.48E-03	
GO:0051055	negative regulation of lipid biosynthetic process	26	5.00E-06	2.78E-03	
GO:0055092	sterol homeostasis	43	5.00E-06	2.32E-03	
GO:0019218	regulation of steroid metabolic process	29	1.00E-05	3.98E-03	
GO:0055088	lipid homeostasis	55	1.00E-05	3.48E-03	
GO:0010894	negative regulation of steroid	22	1.50E-05	4.64E-03	GO:0045939

	biosynthetic process				
GO:0045939	negative regulation of steroid metabolic process	22	1.50E-05	4.64E-03	GO:0010894
GO:0001764	neuron migration	61	2.00E-05	5.57E-03	
GO:0050810	regulation of steroid biosynthetic process	25	2.50E-05	6.33E-03	
GO:0045833	negative regulation of lipid metabolic process	30	3.00E-05	6.96E-03	
GO:0046890	regulation of lipid biosynthetic process	38	4.50E-05	9.63E-03	
GO:0019216	regulation of lipid metabolic process	61	9.00E-05	1.79E-02	
GO:0010565	regulation of cellular ketone metabolic process	33	2.35E-04	4.36E-02	
GO:0003707	steroid hormone receptor activity	14	5.40E-04	9.39E-02	
GO:0038024	cargo receptor activity	64	5.55E-04	9.09E-02	
GO:0060612	adipose tissue development	18	6.00E-04	9.28E-02	
GO:0005319	lipid transporter activity	43	6.05E-04	8.86E-02	

References

Al-Horani F, Al-Moghrabi S, De Beer D (2003) The mechanism of calcification and its relation to photosynthesis and respiration in the scleractinian coral Galaxea fascicularis. Marine Biology, 142, 419-426.

Albright R (2011) Reviewing the effects of ocean acidification on sexual reproduction and early life history stages of reef-building corals. Journal of Marine Biology, 2011.

Allemand D, Ferrier-Pagès C, Furla P *et al.* (2004) Biomineralisation in reef-building corals: from molecular mechanisms to environmental control. Comptes Rendus Palevol, 3, 453-467.

Allemand D, Tambutté É, Zoccola D, Tambutté S (2011) Coral calcification, cells to reefs. In: *Coral reefs: an ecosystem in transition.* pp Page., Springer.

Alvarez BV, Vilas GL, Casey JR (2005) Metabolon disruption: a mechanism that regulates bicarbonate transport. The EMBO journal, 24, 2499-2511.

Anders S, Huber W (2010) Differential expression analysis for sequence count data. Genome biology, 11, R106.

Andersson AJ (2015) A fundamental paradigm for coral reef carbonate sediment dissolution. Frontiers in Marine Science, 2, 52.

Andersson AJ, Kline DI, Edmunds PJ *et al.* (2015) Understanding ocean acidification impacts on organismal to ecological scales. Oceanography, 28, 16-27.

Angell RW (1980) Test morphogenesis (chamber formation) in the foraminifer Spiroloculina hyalina Schulze. The Journal of Foraminiferal Research, 10, 89-101.

Back W, Hanshaw BB (1970) Comparison of chemical hydrogeology of the carbonate peninsulas of Florida and Yucatan. Journal of Hydrology, 10, 330-368.

Back W, Hanshaw BB, Pyle TE, Plummer LN, Weidie A (1979) Geochemical significance of groundwater discharge and carbonate solution to the formation of Caleta Xel Ha, Quintana Roo, Mexico. Water Resources Research, 15, 1521-1535.

Barnes DJ (1970) Coral skeletons: an explanation of their growth and structure. Science, 170, 1305-1308.

Barshis DJ, Ladner JT, Oliver TA, Seneca FO, Traylor-Knowles N, Palumbi SR (2013) Genomic basis for coral resilience to climate change. Proceedings of the National Academy of Sciences, 110, 1387-1392.

Beddows PA, Smart P, Whitaker F, Smith S (2002) Density stratified groundwater circulation on the Caribbean Coast of Yucatan peninsula, Mexico. In: *Karst Waters Institute Special Publication 7: Hydrogeology and Biology of Post-Paleozoic Carbonate Aquifers.* pp Page.

Benjamini Y, Hochberg Y (1995) Controlling the false discovery rate: a practical and powerful approach to multiple testing. Journal of the royal statistical society. Series B (Methodological), 289-300.

Bentov S, Brownlee C, Erez J (2009) The role of seawater endocytosis in the biomineralization process in calcareous foraminifera. Proceedings of the National Academy of Sciences, 106, 21500-21504.

Bernhard JM, Barry JP, Buck KR, Starczak VR (2009) Impact of intentionally injected carbon dioxide hydrate on deep-sea benthic foraminiferal survival. Global Change Biology, 15, 2078-2088.

Blanchon P, Shaw J (1995) Reef drowning during the last deglaciation: evidence for catastrophic sea-level rise and ice-sheet collapse. Geology, 23, 4-8.

Brasier MD (1980) *Microfossils*, G. Allen & Unwin London.

Caldeira K, Wickett ME (2003) Oceanography: anthropogenic carbon and ocean pH. Nature, 425, 365.

Caldeira K, Wickett ME (2005) Ocean model predictions of chemistry changes from carbon dioxide emissions to the atmosphere and ocean. Journal of Geophysical Research: Oceans, 110.

Carricart-Ganivet JP, Merino M (2001) Growth responses of the reef-building coral Montastraea annularis along a gradient of continental influence in the southern Gulf of Mexico. Bulletin of Marine Science, 68, 133-146.

Chan NC, Connolly SR (2013) Sensitivity of coral calcification to ocean acidification: a meta-analysis. Global Change Biology, 19, 282-290.

Chiang JY (2009) Bile acids: regulation of synthesis. Journal of lipid research, 50, 1955-1966.

Cohen AL, Holcomb M (2009) Why corals care about ocean acidification: uncovering the mechanism. Oceanography, 22, 118-127.

Cohen AL, Mcconnaughey TA (2003) Geochemical perspectives on coral mineralization. Reviews in Mineralogy and Geochemistry, 54, 151-187.

Cohen AL, Mccorkle DC, De Putron S, Gaetani GA, Rose KA (2009) Morphological and compositional changes in the skeletons of new coral recruits reared in acidified seawater: Insights into the biomineralization response to ocean acidification. Geochemistry, Geophysics, Geosystems, 10.

Comeau S, Edmunds P, Spindel N, Carpenter R (2014) Fast coral reef calcifiers are more sensitive to ocean acidification in short-term laboratory incubations. Limnology and Oceanography, 59, 1081-1091.

Comeau S, Edmunds PJ, Spindel N, Carpenter RC (2013) The responses of eight coral reef calcifiers to increasing partial pressure of CO2 do not exhibit a tipping point. Limnology and Oceanography, 58, 388-398.

Cordat E, Casey JR (2009) Bicarbonate transport in cell physiology and disease. Biochemical Journal, 417, 423-439.

Crawley A, Kline DI, Dunn S, Anthony K, Dove S (2010) The effect of ocean acidification on symbiont photorespiration and productivity in Acropora formosa. Global Change Biology, 16, 851-863.

Crevison H, Hallock P (2001) Foraminifera as Bioindicators: Key Subtropical Western Atlantic and Caribbean Taxa. University of South Florida, St. Petersburg, FL. Available online at: www. marine. usf. edu/reefslab/foramcd/html_files/titlepage. htm (accessed 2011).

Crook E, Potts D, Rebolledo-Vieyra M, Hernandez L, Paytan A (2012) Calcifying coral abundance near low-pH springs: implications for future ocean acidification. Coral Reefs, 31, 239-245.

Crook ED, Cohen AL, Rebolledo-Vieyra M, Hernandez L, Paytan A (2013) Reduced calcification and lack of acclimatization by coral colonies growing in areas of

persistent natural acidification. Proceedings of the National Academy of Sciences, 110, 11044-11049.

Crook ED, Kroeker KJ, Potts DC, Rebolledo-Vieyra M, Hernandez-Terrones LM, Paytan A (2016) Recruitment and succession in a tropical benthic community in response to in-situ ocean acidification. PLoS ONE, 11, e0146707.

Culver SJ, Lipps JH (2003) Predation on and by Foraminifera. In: *Predator—Prey Interactions in the Fossil Record.* pp Page., Springer.

D'orbigny A (1839) *Foraminifères*, A. Bertrand.

Davies PS (1989) Short-term growth measurements of corals using an accurate buoyant weighing technique. Marine Biology, 101, 389-395.

Davies SW, Marchetti A, Ries JB, Castillo KD (2016) Thermal and pCO2 stress elicit divergent transcriptomic responses in a resilient coral. Frontiers in Marine Science, 3, 112.

Davis CV, Rivest EB, Hill TM, Gaylord B, Russell AD, Sanford E (2017) Ocean acidification compromises a planktic calcifier with implications for global carbon cycling. Scientific Reports, 7, 2225.

De Nooijer LJ, Spero H, Erez J, Bijma J, Reichart G-J (2014) Biomineralization in perforate foraminifera. Earth-Science Reviews, 135, 48-58.

De Nooijer LJ, Toyofuku T, Kitazato H (2009) Foraminifera promote calcification by elevating their intracellular pH. Proceedings of the National Academy of Sciences, pnas. 0904306106.

De Putron SJ, Mccorkle DC, Cohen AL, Dillon A (2011) The impact of seawater saturation state and bicarbonate ion concentration on calcification by new recruits of two Atlantic corals. Coral Reefs, 30, 321-328.

De Wit P, Pespeni MH, Ladner JT *et al.* (2012) The simple fool's guide to population genomics via RNA-Seq: an introduction to high-throughput sequencing data analysis. Molecular Ecology Resources, 12, 1058-1067.

Decarlo TM, Cohen AL, Barkley HC *et al.* (2015) Coral macrobioerosion is accelerated by ocean acidification and nutrients. Geology, 43, 7-10.

Dias B, Hart M, Smart C, Hall-Spencer J (2010) Modern seawater acidification: the response of foraminifera to high-CO2 conditions in the Mediterranean Sea. Journal of the Geological Society, 167, 843-846.

Dickson A, Millero F (1987) A comparison of the equilibrium constants for the dissociation of carbonic acid in seawater media. Deep Sea Research Part A. Oceanographic Research Papers, 34, 1733-1743.

Dickson AG, Sabine CL, Christian JR (2007) *Guide to best practices for ocean CO2 measurements*, North Pacific Marine Science Organization.

Dixon P (2003) VEGAN, a package of R functions for community ecology. Journal of Vegetation Science, 14, 927-930.

Doo SS, Fujita K, Byrne M, Uthicke S (2014) Fate of calcifying tropical symbiont-bearing large benthic foraminifera: living sands in a changing ocean. The Biological Bulletin, 226, 169-186.

Edmunds PJ, Brown D, Moriarty V (2012) Interactive effects of ocean acidification and temperature on two scleractinian corals from Moorea, French Polynesia. Global Change Biology, 18, 2173-2183.

Erez J (2003) The source of ions for biomineralization in foraminifera and their implications for paleoceanographic proxies. Reviews in Mineralogy and Geochemistry, 54, 115-149.

Fabricius KE, Langdon C, Uthicke S *et al.* (2011) Losers and winners in coral reefs acclimatized to elevated carbon dioxide concentrations. Nature Climate Change, 1, 165.

Fabry VJ, Seibel BA, Feely RA, Orr JC (2008) Impacts of ocean acidification on marine fauna and ecosystem processes. ICES Journal of Marine Science, 65, 414-432.

Fantazzini P, Mengoli S, Pasquini L *et al.* (2015) Gains and losses of coral skeletal porosity changes with ocean acidification acclimation. Nature Communications, 6, 7785.

Fine M, Loya Y (2002) Endolithic algae: an alternative source of photoassimilates during coral bleaching. Proceedings of the Royal Society B: Biological Sciences, 269, 1205.

Fine M, Tchernov D (2007) Scleractinian coral species survive and recover from decalcification. Science, 315, 1811-1811.

Form AU, Riebesell U (2012) Acclimation to ocean acidification during long-term CO2 exposure in the cold-water coral Lophelia pertusa. Global Change Biology, 18, 843-853.

Fujita K, Hikami M, Suzuki A, Kuroyanagi A, Sakai K, Kawahata H, Nojiri Y (2011) Effects of ocean acidification on calcification of symbiont-bearing reef foraminifers. Biogeosciences, 8, 2089-2098.

Furla P, Galgani I, Durand I, Allemand D (2000) Sources and mechanisms of inorganic carbon transport for coral calcification and photosynthesis. Journal of Experimental Biology, 203, 3445-3457.

Gattuso J-P, Allemand D, Frankignoulle M (1999) Photosynthesis and calcification at cellular, organismal and community levels in coral reefs: a review on interactions and control by carbonate chemistry. American Zoologist, 39, 160-183.

Gattuso J-P, Frankignoulle M, Bourge I, Romaine S, Buddemeier R (1998) Effect of calcium carbonate saturation of seawater on coral calcification. Global and Planetary Change, 18, 37-46.

Geerken E, Nooijer LJD, Dijk IV, Reichart G-J (2018) Impact of salinity on element incorporation in two benthic foraminiferal species with contrasting magnesium contents. Biogeosciences, 15, 2205-2218.

Gischler E, Möder A (2009) Modern benthic foraminifera on Banco Chinchorro, Quintana Roo, Mexico. Facies, 55, 27-35.

Glas MS, Langer G, Keul N (2012) Calcification acidifies the microenvironment of a benthic foraminifer (Ammonia sp.). Journal of Experimental Marine Biology and Ecology, 424, 53-58.

Gnaiger E, Bitterlich G (1984) Proximate biochemical composition and caloric content calculated from elemental CHN analysis: a stoichiometric concept. Oecologia, 62, 289-298.

Grabherr MG, Haas BJ, Yassour M *et al.* (2011) Full-length transcriptome assembly from RNA-Seq data without a reference genome. Nature biotechnology, 29, 644.

Guinotte JM, Fabry VJ (2008) Ocean acidification and its potential effects on marine ecosystems. Annals of the New York Academy of Sciences, 1134, 320-342.

Hain M, Sigman D, Haug G (2014) 8.18–The biological Pump in the Past. Reference Module in Earth Systems and Environmental Sciences, Treatise on Geochemistry (Second Edition), The Oceans and Marine Geochemistry, 8, 485-517.

Hall-Spencer JM, Rodolfo-Metalpa R, Martin S *et al.* (2008) Volcanic carbon dioxide vents show ecosystem effects of ocean acidification. Nature, 454, 96.

Hallock P (1985) Why are larger foraminifera large? Paleobiology, 11, 195-208.

Hallock P (2000) Symbiont-bearing foraminifera: harbingers of global change? Micropaleontology, 95-104.

Hallock P, Cottey TL, Forward LB, Halas J (1986) Population biology and sediment production of Archaias angulatus (Foraminiferida) in Largo Sound, Florida. The Journal of Foraminiferal Research, 16, 1-8.

Hallock P, Glenn EC (1986) Larger foraminifera: a tool for paleoenvironmental analysis of Cenozoic carbonate depositional facies. Palaios, 55-64.

Hallock P, Peebles MW (1993) Foraminifera with chlorophyte endosymbionts: habitats of six species in the Florida Keys. Marine Micropaleontology, 20, 277-292.

Haynert K, Schönfeld J, Riebesell U, Polovodova I (2011) Biometry and dissolution features of the benthic foraminifer Ammonia aomoriensis at high pCO2. Marine Ecology Progress Series, 432, 53-67.

Hemleben C, Erson O, Berthold W, Spindler M (1986) Calcification and chamber formation in Foraminifera-a brief overview. pp Page.

Henehan MJ, Evans D, Shankle M *et al.* (2017) Size-dependent response of foraminiferal calcification to seawater carbonate chemistry. Biogeosciences (BG), 14, 3287-3308.

Highsmith RC (1979) Coral growth rates and environmental control of density banding. Journal of Experimental Marine Biology and Ecology, 37, 105-125.

Hikami M, Ushie H, Irie T *et al.* (2011) Contrasting calcification responses to ocean acidification between two reef foraminifers harboring different algal symbionts. Geophysical Research Letters, 38.

Hoegh-Guldberg O (1999) Climate change, coral bleaching and the future of the world's coral reefs. Marine and Freshwater Research, 50, 839-866.

Hoegh-Guldberg O, Mumby PJ, Hooten AJ *et al.* (2007) Coral reefs under rapid climate change and ocean acidification. Science, 318, 1737-1742.

Hofmann GE, Smith JE, Johnson KS *et al.* (2011) High-frequency dynamics of ocean pH: a multi-ecosystem comparison. PLoS ONE, 6, e28983.

Holmen SL, Giambernardi TA, Zylstra CR *et al.* (2004) Decreased BMD and limb deformities in mice carrying mutations in both Lrp5 and Lrp6. Journal of Bone and Mineral Research, 19, 2033-2040.

Hönisch B, Hemming NG (2004) Ground-truthing the boron isotope-paleo-pH proxy in planktonic foraminifera shells: Partial dissolution and shell size effects. Paleoceanography, 19.

Horton BP, Murray JW (2007) The roles of elevation and salinity as primary controls on living foraminiferal distributions: Cowpen Marsh, Tees Estuary, UK. Marine Micropaleontology, 63, 169-186.

Houten SM, Wanders RJ (2010) A general introduction to the biochemistry of mitochondrial fatty acid β-oxidation. Journal of inherited metabolic disease, 33, 469-477.

Hughes TP, Kerry JT, Baird AH *et al.* (2018) Global warming transforms coral reef assemblages. Nature, 556, 492.

Jeffrey ST, Humphrey G (1975) New spectrophotometric equations for determining chlorophylls a, b, c1 and c2 in higher plants, algae and natural phytoplankton. Biochemie und Physiologie der Pflanzen, 167, 191-194.

Jokiel P, Maragos J (1978) Coral growth: buoyant weight technique. UNESCO, Paris, France.

Jokiel PL (2011) The reef coral two compartment proton flux model: A new approach relating tissue-level physiological processes to gross corallum morphology. Journal of Experimental Marine Biology and Ecology, 409, 1-12.

Jury CP, Whitehead RF, Szmant AM (2010) Effects of variations in carbonate chemistry on the calcification rates of Madracis auretenra (= Madracis mirabilis sensu Wells, 1973): bicarbonate concentrations best predict calcification rates. Global Change Biology, 16, 1632-1644.

Kang KS, Robling AG (2015) New insights into Wnt–Lrp5/6–β-catenin signaling in mechanotransduction. Frontiers in endocrinology, 5, 246.

Kaniewska P, Campbell PR, Kline DI, Rodriguez-Lanetty M, Miller DJ, Dove S, Hoegh-Guldberg O (2012) Major cellular and physiological impacts of ocean acidification on a reef building coral. PLoS ONE, 7, e34659.

Kenkel C, Meyer E, Matz M (2013) Gene expression under chronic heat stress in populations of the mustard hill coral (P orites astreoides) from different thermal environments. Molecular Ecology, 22, 4322-4334.

Kenkel CD, Moya A, Strahl J, Humphrey C, Bay LK (2018) Functional genomic analysis of corals from natural CO2-seeps reveals core molecular responses involved in acclimatization to ocean acidification. Global Change Biology, 24, 158-171.

Keul N, Langer G, De Nooijer LJ, Bijma J (2013) Effect of ocean acidification on the benthic foraminifera Ammonia sp. is caused by a decrease in carbonate ion concentration. Biogeosciences, 10, 6185-6198.

Kleypas JA, Buddemeier RW, Archer D, Gattuso J-P, Langdon C, Opdyke BN (1999) Geochemical consequences of increased atmospheric carbon dioxide on coral reefs. Science, 284, 118-120.

Knorr PO, Robbins LL, Harries PJ, Hallock P, Wynn J (2015) Response of the miliolid Archaias angulatus to simulated ocean acidification. The Journal of Foraminiferal Research, 45, 109-127.

Kokubu C, Heinzmann U, Kokubu T *et al.* (2004) Skeletal defects in ringelschwanz mutant mice reveal that Lrp6 is required for proper somitogenesis and osteogenesis. Development, 131, 5469-5480.

Krief S, Hendy EJ, Fine M, Yam R, Meibom A, Foster GL, Shemesh A (2010) Physiological and isotopic responses of scleractinian corals to ocean acidification. Geochimica Et Cosmochimica Acta, 74, 4988-5001.

Kroeker KJ, Kordas RL, Crim RN, Singh GG (2010) Meta-analysis reveals negative yet variable effects of ocean acidification on marine organisms. Ecology Letters, 13, 1419-1434.

Ladner JT, Palumbi SR (2012) Extensive sympatry, cryptic diversity and introgression throughout the geographic distribution of two coral species complexes. Molecular Ecology, 21, 2224-2238.

Lajeunesse TC, Parkinson JE, Gabrielson PW, Jeong HJ, Reimer JD, Voolstra CR, Santos SR (2018) Systematic revision of Symbiodiniaceae highlights the antiquity and diversity of coral endosymbionts. Current Biology, 28, 2570-2580. e2576.

Lee K, Kim Y, Lee S-J *et al.* (2013) MDGAs interact selectively with neuroligin-2 but not other neuroligins to regulate inhibitory synapse development. Proceedings of the National Academy of Sciences, 110, 336-341.

Legendre L, Le Fèvre J (1995) Microbial food webs and the export of biogenic carbon in oceans. Aquatic Microbial Ecology, 9, 69-77.

Lenz EA, Edmunds PJ (2017) Branches and plates of the morphologically plastic coral Porites rus are insensitive to ocean acidification and warming. Journal of Experimental Marine Biology and Ecology, 486, 188-194.

Lesser MP, Mazel CH, Gorbunov MY, Falkowski PG (2004) Discovery of symbiotic nitrogen-fixing cyanobacteria in corals. Science, 305, 997-1000.

Lough J, Barnes D (1989) Possible relationships between environmental variables and skeletal density in a coral colony from the central Great Barrier Reef. Journal of Experimental Marine Biology and Ecology, 134, 221-241.

Lough J, Barnes D (2000) Environmental controls on growth of the massive coral Porites. Journal of Experimental Marine Biology and Ecology, 245, 225-243.

Loya Y, Sakai K, Yamazato K, Nakano Y, Sambali H, Van Woesik R (2001) Coral bleaching: the winners and the losers. Ecology Letters, 4, 122-131.

Lueker TJ, Dickson AG, Keeling CD (2000) Ocean pCO2 calculated from dissolved inorganic carbon, alkalinity, and equations for K1 and K2: validation based on laboratory measurements of CO2 in gas and seawater at equilibrium. Marine Chemistry, 70, 105-119.

Mani A, Radhakrishnan J, Wang H *et al.* (2007) LRP6 mutation in a family with early coronary disease and metabolic risk factors. Science, 315, 1278-1282.

Manzello D (2010) Coral growth with thermal stress and ocean acidification: lessons from the eastern tropical Pacific. Coral Reefs, 29, 749-758.

Manzello DP, Kleypas JA, Budd DA, Eakin CM, Glynn PW, Langdon C (2008) Poorly cemented coral reefs of the eastern tropical Pacific: Possible insights into reef development in a high-CO2 world. Proceedings of the National Academy of Sciences.

Martin M (2011) Cutadapt removes adapter sequences from high-throughput sequencing reads. EMBnet. journal, 17, pp. 10-12.

Martin RE (1986) Habitat and distribution of the foraminifer Archaias angulatus (Fichtel and Moll)(Miliolina, Soritidae), northern Florida Keys. The Journal of Foraminiferal Research, 16, 201-206.

Mcconnaughey T, Whelan J (1997) Calcification generates protons for nutrient and bicarbonate uptake. Earth-Science Reviews, 42, 95-117.

Mcintyre-Wressnig A, Bernhard JM, Mccorkle DC, Hallock P (2013) Non-lethal effects of ocean acidification on the symbiont-bearing benthic foraminifer Amphistegina gibbosa. Marine Ecology Progress Series, 472, 45-60.

Mclusky DS, Elliott M, Elliott M (2004) *The estuarine ecosystem: ecology, threats and management*, Oxford University Press on Demand.

Mehrbach C, Culberson C, Hawley J, Pytkowicx R (1973) Measurement of the apparent dissociation constants of carbonic acid in seawater at atmospheric pressure1. Limnology and Oceanography, 18, 897-907.

Mollica NR, Guo W, Cohen AL, Huang K-F, Foster GL, Donald HK, Solow AR (2018) Ocean acidification affects coral growth by reducing skeletal density. Proceedings of the National Academy of Sciences, 115, 1754-1759.

Morse JW, Andersson AJ, Mackenzie FT (2006) Initial responses of carbonate-rich shelf sediments to rising atmospheric pCO2 and "ocean acidification": Role of high Mg-calcites. Geochimica Et Cosmochimica Acta, 70, 5814-5830.

Moya A, Huisman L, Ball E *et al.* (2012) Whole transcriptome analysis of the coral Acropora millepora reveals complex responses to CO2-driven acidification during the initiation of calcification. Molecular Ecology, 21, 2440-2454.

Moya A, Huisman L, Foret S, Gattuso JP, Hayward DC, Ball E, Miller DJ (2015) Rapid acclimation of juvenile corals to CO2-mediated acidification by upregulation of heat shock protein and Bcl-2 genes. Molecular Ecology, 24, 438-452.

Muller PH (1974) Sediment production and population biology of the benthic foraminifer Amphistegina madagascariensis 1, 2. Limnology and Oceanography, 19, 802-809.

Murray JW (1991) Ecology and distribution of benthic foraminifera. Biology of foraminifera, 221-254.

Nehrke G, Keul N, Langer G, De Nooijer L, Bijma J, Meibom A (2013) A new model for biomineralization and trace-element signatures of Foraminifera tests. Biogeosciences, 10, 6759-6767.

Null KA, Knee KL, Crook ED, De Sieyes NR, Rebolledo-Vieyra M, Hernández-Terrones L, Paytan A (2014) Composition and fluxes of submarine groundwater along the Caribbean coast of the Yucatan Peninsula. Continental Shelf Research, 77, 38-50.

Ogawa D, Bobeszko T, Ainsworth T, Leggat W (2013) The combined effects of temperature and CO 2 lead to altered gene expression in Acropora aspera. Coral Reefs, 32, 895-907.

Oksanen J, Blanchet FG, Kindt R *et al.* (2013) Package 'vegan'. Community ecology package, version, 2.

Orr JC, Fabry VJ, Aumont O *et al.* (2005) Anthropogenic ocean acidification over the twenty-first century and its impact on calcifying organisms. Nature, 437, 681.

Paytan A, Crook ED, Cohen AL, Martz TR, Takashita Y, Rebolledo-Vieyra M, Hernandez L (2014) Reply to Iglesias-Prieto et al.: Combined field and laboratory approaches for the study of coral calcification. Proceedings of the National Academy of Sciences, 111, E302-E303.

Pettit L, Hart M, Medina-Sánchez A, Smart C, Rodolfo-Metalpa R, Hall-Spencer J, Prol-Ledesma R (2013) Benthic foraminifera show some resilience to ocean acidification in the northern Gulf of California, Mexico. Marine Pollution Bulletin, 73, 452-462.

Pierrot D, Lewis E, Wallace D (2006) MS Excel program developed for CO2 system calculations. ORNL/CDIAC-105a. Carbon Dioxide Information Analysis Center, Oak Ridge National Laboratory, US Department of Energy, Oak Ridge, Tennessee.

Poag CW (1981) Ecologic atlas of benthic foraminifera of the Gulf of Mexico.

Raven J, Caldeira K, Elderfield H *et al.* (2005) *Ocean acidification due to increasing atmospheric carbon dioxide*, The Royal Society.

Reynaud S, Leclercq N, Romaine-Lioud S, Ferrier-Pagés C, Jaubert J, Gattuso JP (2003) Interacting effects of CO2 partial pressure and temperature on photosynthesis and calcification in a scleractinian coral. Global Change Biology, 9, 1660-1668.

Ries JB, Cohen AL, Mccorkle DC (2009) Marine calcifiers exhibit mixed responses to CO2-induced ocean acidification. Geology, 37, 1131-1134.

Rocker MM, Noonan S, Humphrey C, Moya A, Willis BL, Bay LK (2015) Expression of calcification and metabolism-related genes in response to elevated pCO 2

and temperature in the reef-building coral Acropora millepora. Marine Genomics, 24, 313-318.

Rodolfo-Metalpa R, Houlbrèque F, Tambutté É *et al.* (2011) Coral and mollusc resistance to ocean acidification adversely affected by warming. Nature Climate Change, 1, 308.

Rodolfo-Metalpa R, Martin S, Ferrier-Pagès C, Gattuso J-P (2010) Response of the temperate coral Cladocora caespitosa to mid-and long-term exposure to pCO 2 and temperature levels projected for the year 2100 AD. Biogeosciences, 7, 289-300.

Russell DW (2003) The enzymes, regulation, and genetics of bile acid synthesis. Annual review of biochemistry, 72, 137-174.

Sabine CL, Feely RA, Gruber N *et al.* (2004) The oceanic sink for anthropogenic CO2. Science, 305, 367-371.

Schmiedl G, Mackensen A, Müller P (1997) Recent benthic foraminifera from the eastern South Atlantic Ocean: dependence on food supply and water masses. Marine Micropaleontology, 32, 249-287.

Schmitz G, Langmann T (2001) Structure, function and regulation of the ABC1 gene product. Current opinion in lipidology, 12, 129-140.

Schoepf V, Grottoli AG, Warner ME *et al.* (2013) Coral energy reserves and calcification in a high-CO2 world at two temperatures. PLoS ONE, 8, e75049.

Sene A, Khan AA, Cox D *et al.* (2013) Impaired cholesterol efflux in senescent macrophages promotes age-related macular degeneration. Cell metabolism, 17, 549-561.

Shapiro H, Kolodziejczyk AA, Halstuch D, Elinav E (2018) Bile acids in glucose metabolism in health and disease. Journal of Experimental Medicine, 215, 383-396.

Smith L, Barshis D, Birkeland C (2007) Phenotypic plasticity for skeletal growth, density and calcification of Porites lobata in response to habitat type. Coral Reefs, 26, 559-567.

Smith SV, Buddemeier R (1992) Global change and coral reef ecosystems. Annual Review of Ecology and Systematics, 23, 89-118.

Stimson J, Kinzie Iii RA (1991) The temporal pattern and rate of release of zooxanthellae from the reef coral Pocillopora damicornis (Linnaeus) under nitrogen-enrichment and control conditions. Journal of Experimental Marine Biology and Ecology, 153, 63-74.

Stocker T (2014) *Climate change 2013: the physical science basis: Working Group I contribution to the Fifth assessment report of the Intergovernmental Panel on Climate Change*, Cambridge University Press.

Tambutté E, Venn A, Holcomb M *et al.* (2015) Morphological plasticity of the coral skeleton under CO 2-driven seawater acidification. Nature Communications, 6, 7368.

Team RC (2015) R: A language and environment for statistical computing.

Ter Kuile B, Erez J (1991) Carbon budgets for two species of benthonic symbiont-bearing foraminifera. The Biological Bulletin, 180, 489-495.

Therneau TM, Lumley T (2015) Package 'survival'. R Top Doc, 128.

Towle EK, Enochs IC, Langdon C (2015) Threatened Caribbean coral is able to mitigate the adverse effects of ocean acidification on calcification by increasing feeding rate. PLoS ONE, 10.

Toyofuku T, Jan De Nooijer L, Yamamoto H, Kitazato H (2008) Real-time visualization of calcium ion activity in shallow benthic foraminiferal cells using the fluorescent indicator Fluo-3 AM. Geochemistry, Geophysics, Geosystems, 9.

Toyofuku T, Matsuo MY, De Nooijer LJ *et al.* (2017) Proton pumping accompanies calcification in foraminifera. Nature Communications, 8, 14145.

Tresguerres M (2016) Novel and potential physiological roles of vacuolar-type H+-ATPase in marine organisms. Journal of Experimental Biology, 219, 2088-2097.

Uppström LR (1974) The boron/chlorinity ratio of deep-sea water from the Pacific Ocean. In: *Deep Sea Research and Oceanographic Abstracts.* pp Page.

Uthicke S, Fabricius KE (2012) Productivity gains do not compensate for reduced calcification under near-future ocean acidification in the photosynthetic benthic foraminifer species Marginopora vertebralis. Global Change Biology, 18, 2781-2791.

Uthicke S, Momigliano P, Fabricius K (2013) High risk of extinction of benthic foraminifera in this century due to ocean acidification. Scientific Reports, 3, 1769.

Van Dijk I, Bernhard JM, De Nooijer LJ, Nehrke G, Wit JC, Reichart G-J (2017) Combined impacts of ocean acidification and dysoxia on survival and growth

of four agglutinating foraminifera. Journal of Foraminiferal Research, 47, 294-303.

Van Oppen MJ, Oliver JK, Putnam HM, Gates RD (2015) Building coral reef resilience through assisted evolution. Proceedings of the National Academy of Sciences, 112, 2307-2313.

Vergnes L, Lee JM, Chin RG, Auwerx J, Reue K (2013) Diet1 functions in the FGF15/19 enterohepatic signaling axis to modulate bile acid and lipid levels. Cell metabolism, 17, 916-928.

Vidal-Dupiol J, Zoccola D, Tambutté E *et al.* (2013) Genes related to ion-transport and energy production are upregulated in response to CO2-driven pH decrease in corals: new insights from transcriptome analysis. PLoS ONE, 8, e58652.

Wantland KF (1967) Recent benthonic foraminifera of the British Honduras shelf. Rice University.

Wickham H (2016) *ggplot2: elegant graphics for data analysis*, Springer.

Zeebe RE, Sanyal A (2002) Comparison of two potential strategies of planktonic foraminifera for house building: Mg2+ or H+ removal? Geochimica Et Cosmochimica Acta, 66, 1159-1169.

Zoccola D, Ganot P, Bertucci A *et al.* (2015) Bicarbonate transporters in corals point towards a key step in the evolution of cnidarian calcification. Scientific Reports, 5, 9983.